Study on the role of neuropeptide receptor VPAC2 overactivation in schizophrenia and its potential therapeutic target

Laboratory of Biopharmaceutics

Graduate School of Pharmaceutical Sciences

Osaka University

Lu Chen

Contents

Introduction

Schizophrenia is a chronic disabling brain disorder affecting approximately 1% of the world's population, and nearly 10% of those with schizophrenia have an affected first-degree relative. Schizophrenia is mainly characterized by positive symptoms such as hallucinations and delusions, negative symptoms such as decreased motivation and cognitive dysfunction (Millan et al., 2016; Owen et al., 2016). Approximately one-third of patients with this diagnosis will attempt suicide, and eventually, about only one in ten of these will be successfully treated. New treatments are needed to lessen the suffering of patients and their families and to decrease the economic cost. The advent of the genomic era has led to the discovery of linkages of several genes and pathways to schizophrenia that may serve as new biomarkers or therapeutic targets for this disease. Accumulating evidence indicates that a number of rare copy number variants (CNVs), including both deletions and duplications, have been strongly associated with schizophrenia (Foley et al., 2017; Rosti et al., 2013; Walsh et al., 2008). Additionally, many CNVs found in schizophrenia are also present in autism spectrum disorder (ASD), suggesting that there may be a common molecular basis for both disorders (Kushima et al., 2018). Among the most highly penetrant genetic risk factors for neuropsychiatric disorders, clinical studies have shown that microduplications at 7q36.3, containing *VIPR2*, confer significant risk for schizophrenia (Vacic et al., 2011; Levinson et al., 2011; Yuan et al., 2014; Li et al., 2016; Marshall et al., 2017). *VIPR2* encodes VPAC2, a seven transmembrane heterotrimeric G protein-coupled receptor (GPCR) that binds two homologous neuropeptides with high affinity, vasoactive intestinal peptide (VIP) and pituitary adenylate cyclase-activating polypeptide (PACAP) (Vaudry et al., 2009). PACAP and its receptors (PAC1, VPAC1, and VPAC2) are expressed in various organs, including the sensory, digestive, and reproductive organs, in addition to the central and peripheral nervous systems, and thus PACAP exhibits a variety of biological activities in a distinct manner. VIP binds to two of the three receptors, VPAC1 and VPAC2, with an affinity similar to that of PACAP. VIP has a very low affinity for the PAC1 receptor (IC_{50}: >1,000 nM). Lymphocytes from patients with 7q36.3 microduplications exhibited higher *VIPR2* gene expression and VIP responsiveness (cAMP induction) (Vacic et al., 2011), demonstrating the functional significance of the microduplications. These suggest that overactivation of the VPAC2 receptor signaling is involved in the etiology of schizophrenia and provides large-scale genetic evidence for a specific receptor-mediated (and potentially drug targetable) signaling pathway linked to schizophrenia that is distinct from dopaminergic, glutamatergic, and serotonergic systems. However, the mechanism by which overactive VPAC2 signaling may lead to schizophrenia is unknown. In the present study, to investigate how increased *VIPR2* dosage might predispose to psychiatric disorders, we have tried to develop a bacterial artificial chromosome (BAC) transgenic mouse model of *VIPR2* CNV that recapitulates the genetic architecture of the susceptibility allele

(Chapter 1). Furthermore, since the VPAC2 receptor is considered an attractive drug target for development to treat schizophrenia, we have tried in another study to develop a selective VPAC2 receptor antagonist peptide (Chapter 2).

Chapter 1 Development of a bacterial artificial chromosome transgenic mouse model of *VIPR2* copy number variation

1.1 Background

CNV is a chromosomal structural variation that manifests as deletions or multiple replications in the genome. As a source of genetic diversity, CNVs are abundant in the human genome (Feuk et al., 2006). Most CNVs are intergenic, minor, or contain genes that can tolerate copy number variation and are benign. However, several recent genome-wide association studies (GWAS) have identified multiple associated disorders and possible chronic CNVs that convincingly increase the risk of neurodevelopmental disorders such as schizophrenia, ASD, intellectual disability, and attention-deficit hyperactivity disorder (Malhotra and Sebat, 2012). Most CNVs contain many genes that affect multiple organ systems and brain regions at different developmental stages. It is difficult to distinguish between cell type autonomy and systemic effects. Currently, there are significant gaps in linking these candidate genetic vulnerabilities to dysfunctional neuronal subtypes and circuits. Etiologically relevant animal models and complex genetic dissections are needed to confirm the disease causation of CNV and to understand when/where/how CNV affects the development, structure, and function of neural circuits. These studies are necessary to gain insight into disease pathogenesis and pathophysiological mechanisms (Nestler and Hyman, 2010). Previous studies have found microduplications of the *VIPR2* gene to be strongly associated with schizophrenia in genetic studies of CNVs (Levinson et al., 2011; Z. Li et al., 2016; Marshall et al., 2017; Vacic et al., 2011; Yuan et al., 2014). Thus, the aim of this study was to establish an etiologically relevant animal model of one of the CNVs associated with schizophrenia to (i) provide further evidence to support disease causation and (ii) translate genetic vulnerability into mechanistic pathophysiological insights. We tried to develop a bacterial artificial chromosome (BAC) transgenic mouse model of *VIPR2* CNV. BAC is a useful resource for long-range analysis of the genomic organization and gene function. On average, BAC inserts contain 130–200 kb of mouse genomic DNA. Ideally, during BAC transgenesis, BAC DNA introduced by pronuclear injection is integrated as intact BAC molecules into the mouse genome. Transgenic mice containing intact BAC molecules are likely to show physiologically-relevant gene expression patterns and copy number-dependent expression levels.

1.2 Results

1.2.1 Generation of *VIPR2* BAC transgenic mice

Using BAC-mediated transgenic methods, we generated mice with additional integrated copies of the mouse *VIPR2* gene. Potential F0 founder and future progeny were screened by PCR. Southern blot analysis revealed three copies of the transgene in hemizygous F1 generation mice (Fig. 1). Lines with documented germline transgene transmission were maintained by breeding hemizygous transgenic animals to C57BL/6J wild-type animals. Then, expression of VPAC2 receptor mRNA significantly increased in the prefrontal cortex, cerebral cortex, and hippocampus of VIPR2 BAC transgenic (Tg) mice (F2 generation) compared with wild-type

littermates (Fig. 2). Interestingly, the expression of PAC1 and VPAC1, but not dopamine-D_2, receptor mRNA in the prefrontal cortex of VIPR2 BAC Tg mice was significantly less than that of wild-type mice.

A

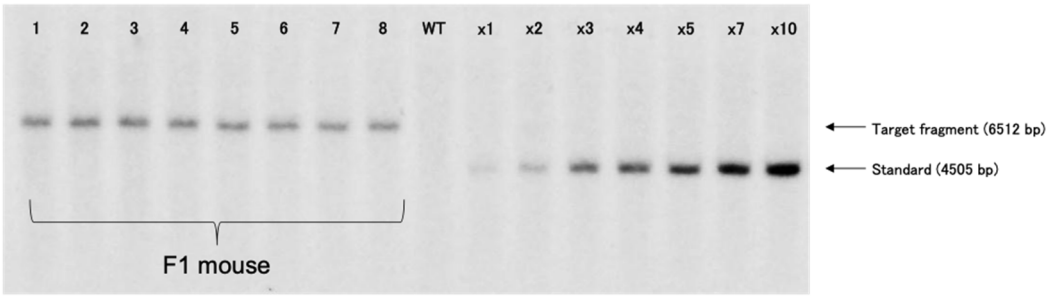

B

Lane No.	ID	Sex	Signal intensity (WT=0)	Copy Number
1	ODA115F1-002(F1)	♂	17.81	3
2	ODA115F1-003(F1)	♂	20.78	3
3	ODA115F1-004(F1)	♂	20.57	3
4	ODA115F1-006(F1)	♀	17.74	3
5	ODA115F1-102(F1)	♂	17.64	3
6	ODA115F1-103(F1)	♂	15.98	3
7	ODA115F1-105(F1)	♀	14.49	3
8	ODA115F1-106(F1)	♀	15.38	3
WT	Wild Type Genome	–	0.00	0
x1	Standard (1copy)	–	3.41	1
x2	Standard (2copy)	–	8.42	2
x3	Standard (3copy)	–	22.89	3
x4	Standard (4copy)	–	29.84	4
x5	Standard (5copy)	–	34.80	5
x7	Standard (7copy)	–	47.663	7
x10	Standard (10copy)	–	65.539	10

Figure 1. Copy number validation of the transgene in F1 mice. The copy numbers of the transgene were measured by Southern blot analysis of DNA isolated from the tails of the F1 mice.

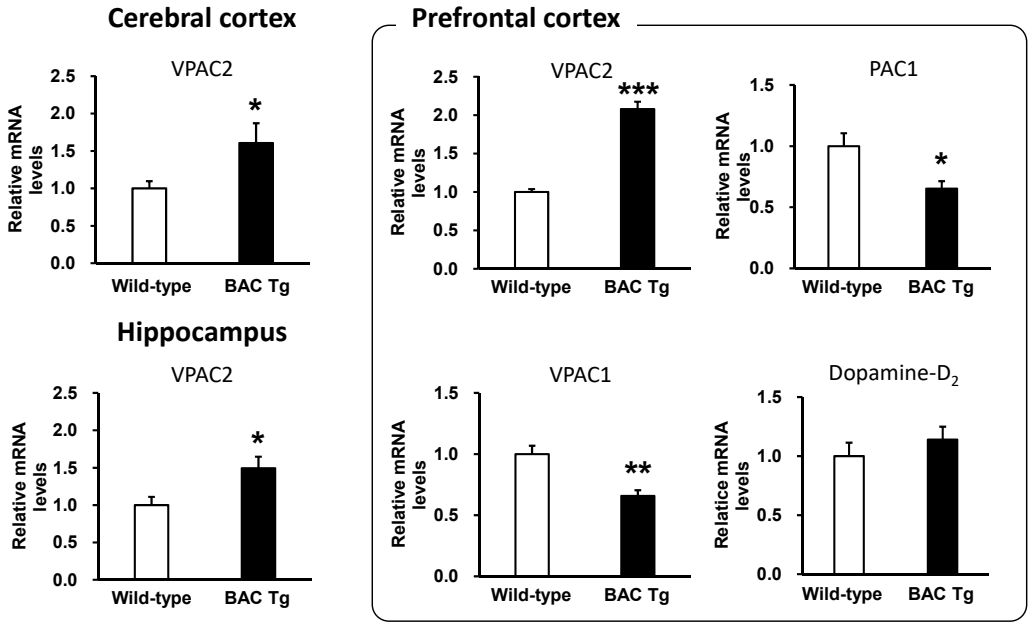

Figure 2. PAC1, VPAC1, VPAC2 mRNA expression in the brain of F2 BAC Tg mice. Results are expressed as the mean ± SEM of 5 mice. *$P < 0.05$, **$P < 0.01$, ***$P < 0.001$, compared with wild-type.

1.2.2 Behavioral analysis

We next investigated several behaviors relevant to schizophrenia and ASD in VIPR2 BAC Tg mice. The prepulse inhibition (PPI) test provides an operational measure of the sensorimotor gating system, which is impaired in patients with schizophrenia (Amann et al., 2010; Mena et al., 2016). In VIPR2 BAC Tg mice, the percent of the PPI of the startle reflex was significantly lower than that of wild-type littermates (Fig. 3A), indicating impaired sensory-motor gating. There was no difference in the baseline startle response between genotypes (Fig. 3B).

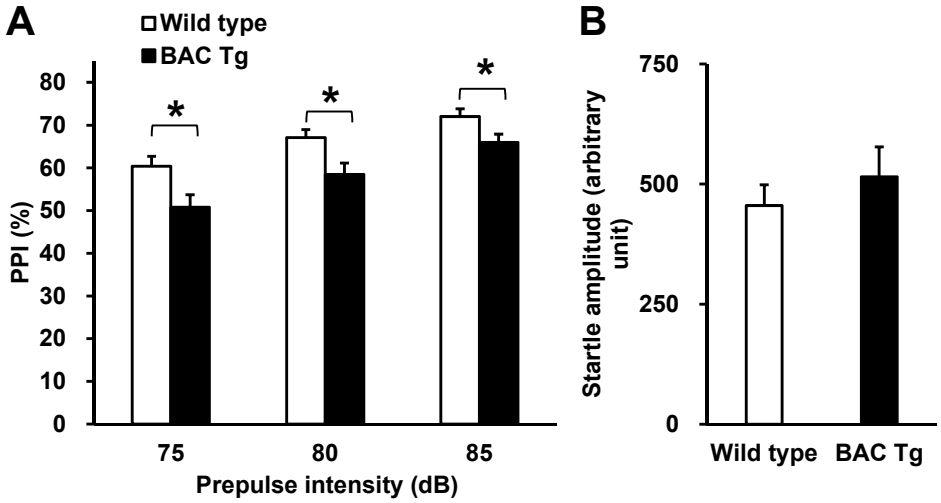

Figure 3. The prepulse inhibition (PPI) test. The percentage of PPI at each prepulse intensity (A) and startle amplitude (B) are shown. Results are expressed as the mean ± SEM of 28-30 mice/group. $^{*}P < 0.05$, compared with wild-type.

In the brain, the VPAC2 receptor is highly expressed in neurons in the thalamus and hypothalamus, especially in the suprachiasmatic nuclei, as well as the cerebral cortex (Sheward et al., 1995; An et al., 2012). Its role regarding circadian rhythms has been studied extensively using VPAC2-deficient mice and VPAC2-overexpressing mice, demonstrating that the VPAC2 receptor is critically involved in the synchronization of neural activity and the regulation of firing frequency (Shen et al., 2000; Harmar et al., 2002). Additionally, a characteristic of rodent models relevant to schizophrenia has been suggested to be enhanced locomotor activity. To assess this trait, the spontaneous locomotor activity of mice was measured continuously throughout the week (Fig. 4). During the light and dark periods, VIPR2 BAC Tg mice were more active than wild-type mice (Fig. 4A) and showed a significant increase in total locomotor activity (Fig. 4B).

The three-chamber social preference test, which assesses the animal's preference for a social stimulus over a non-social stimulus, is one of the most commonly used methods for evaluating sociability in mouse models of schizophrenia and ASD (Hanks et al., 2013; Silverman et al., 2010). In this test (Fig. 5), subjects generally spent more time on either side of the apparatus than in the middle chamber. Subjects spent more time in the chamber containing the unfamiliar mouse than in the empty side, indicating social preference. However, VIPR2 BAC Tg mice displayed lower social preference than wild-type littermates.

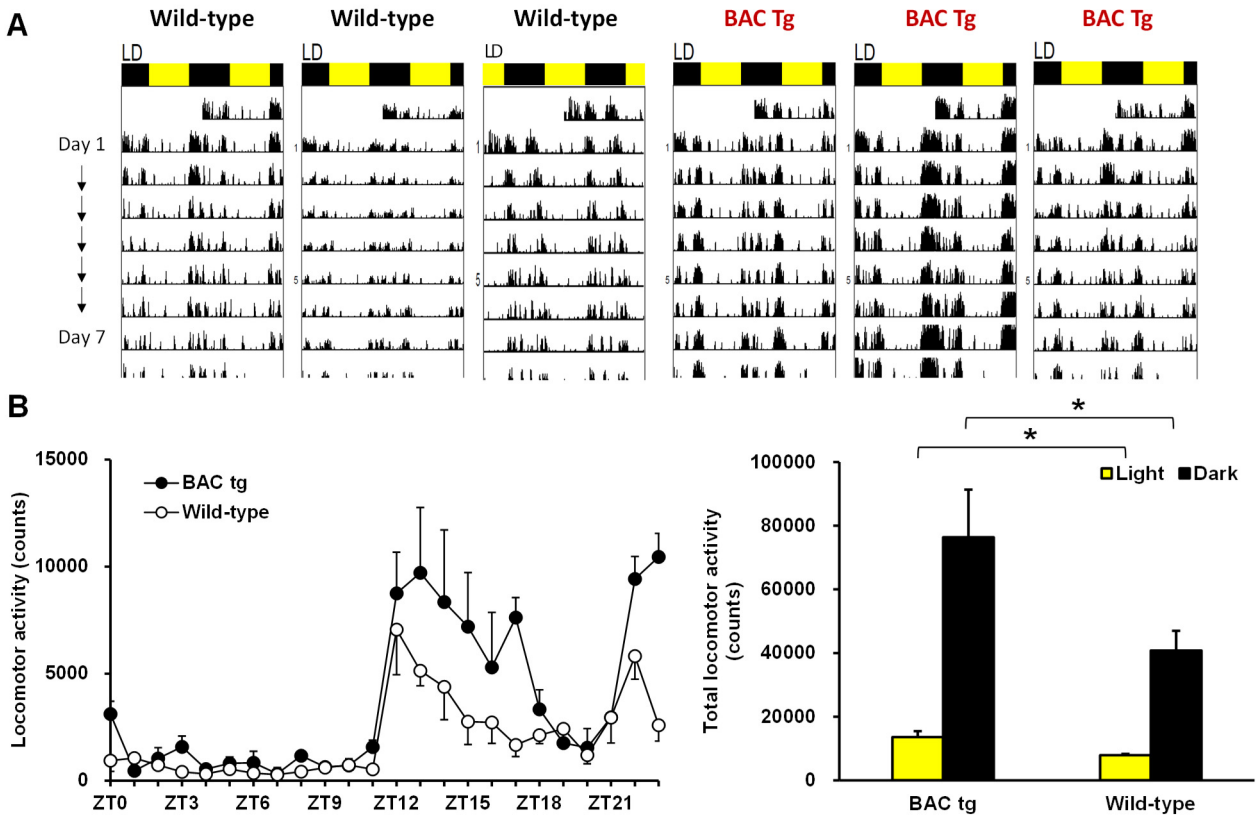

Figure 4. Spontaneous locomotor activity in nocturnal and diurnal periods. Each mouse was housed individually in a wire-topped clear polycarbonate cage in the soundproof box under controlled environmental conditions (22 ± 1°C; 12:12-h light/dark cycle, lights on at 0800 h; food and water *ad libitum*) for 1 week. (A) Representative actograms of motor activity for wild-type and VIPR2 BAC Tg mice. (B) Time-course and total locomotor activity of mice during light and dark periods on day 7 are shown. Results are expressed as the mean ± SEM of 3 mice. $^{*}P < 0.05$, compared with wild-type.

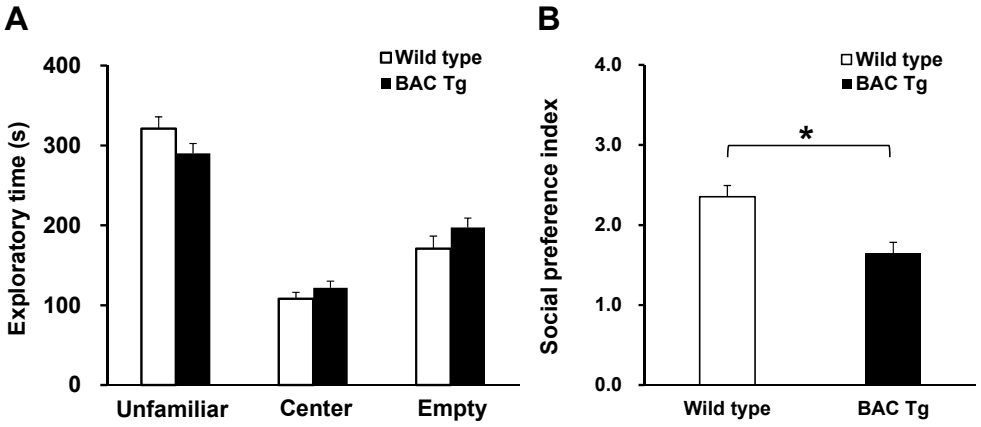

Figure 5. The three-chamber social interaction test. After habituation, a mouse was placed in the central chamber of a clear Plexiglas box divided into three interconnected chambers and was given a choice to interact with either an empty wire cup (Empty) or a similar wire cup with an unfamiliar mouse (Unfamiliar). The amount of time spent in each of the three chambers during a 10-min test (A) and the social preference index (unfamiliar/empty ratio) (B) are shown. Results are expressed as the mean ± SEM of 21-22 mice/group. $^{*}P < 0.05$, compared with wild-type.

Schizophrenia is associated with abnormalities in emotional processing and cognition, which might result from disruption of the underlying neural mechanisms governing emotional learning and memory (Holt et al., 2009). To investigate this possibility in VIPR2 BAC Tg mice, we measured the memory formation, retention, and extinction in the fear conditioning test (Fig. 6). During the training phase of fear conditioning (Day 1), both VIPR2 BAC Tg and wild-type mice had low levels of freezing before training began (Baseline) and froze about 70 % of the time following the training session. There was no significant difference in the acquisition between groups. After the conditioning day, we performed the contextual fear test on Day 2 and the tone-cued fear test on Day 3. There were no significant differences in contextual freezing responses or in tone-cued freezing responses between groups. For the cued extinction on Days 4 and 5, freezing behaviors of mice were gradually decreased and then reached a similar level as the baseline. There was no significant difference in freezing responses between groups.

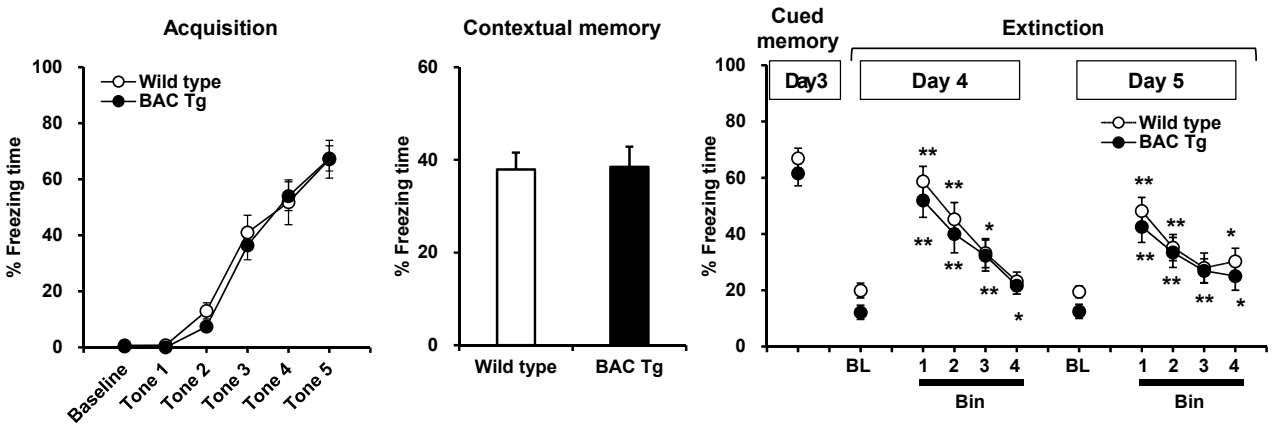

Figure 6. The fear conditioning test. On Day 1, mice were trained with five tone-shock pairings. Then, mice were subjected to the contextual fear memory test on Day 2, cued fear memory test, and cued fear extinction paradigm from Days 3 to 5. Results are expressed as the mean ± SEM of 16-22 mice/group. $^{*}P < 0.05$, $^{**}P < 0.01$, compared with wild-type. BL; baseline

Cognitive impairments in schizophrenia are among the core symptoms of the disease (Sharma and Antonova, 2003), they correlate with the functional outcome (Fett et al., 2010), and are not well treated with current antipsychotic therapies (Harvey and Keefe, 2001; Keefe et al., 2007). The novel object recognition task is a test paradigm thought to reflect visual learning and recognition processing (Young et al., 2009). During the test session at 24 h after the training session, VIPR2 BAC Tg mice showed a reduction in the time difference spent exploring each object, whereas wild-type mice explored the novel object by a significant preference in the novel object recognition test (Fig. 7A). Additionally, the discrimination index was significantly lower in VIPR2 BAC Tg mice than wild-type mice (Fig. 7B).

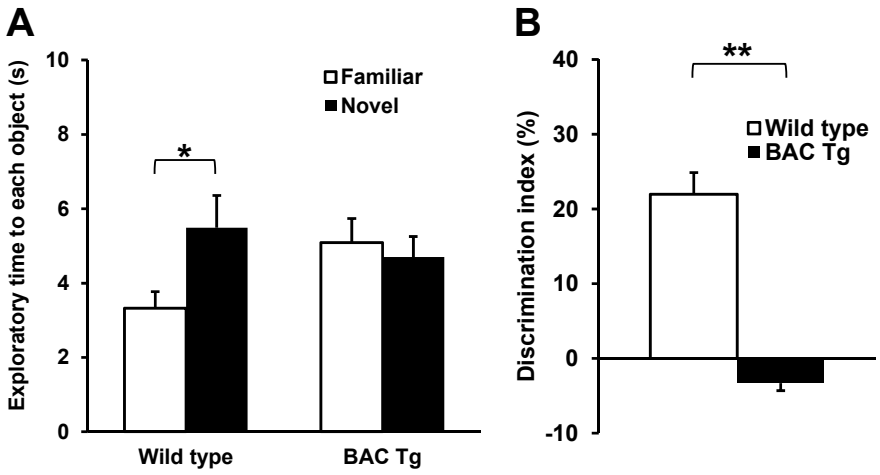

Figure 7. The novel object recognition test. (A) Time spent exploring two objects in the test session. (D) Time spent exploring each object in the test session. (B) The discrimination index (%) was calculated as the difference between the novel and familiar object exploration times divided by the total time spent exploring two objects. Results are expressed as the mean ± SEM of 19-23 mice/group. *$P < 0.05$, **$P < 0.01$.

1.3 Discussion

Analysis of CNV has become an important tool in the identification of novel and important mutations associated with disease and phenotypic traits. While CNVs typically explain only a small proportion of trait heritability, they may have large effects and functional consequences. Therefore, analyses of CNVs have a strong potential to lead to the elucidation of processes involved in the pathogenesis of mental health disorders. We have previously found that repeated administration of the selective VPAC2 receptor agonist Ro 25-1553 to newborn mice reduced synaptic proteins synaptophysin and postsynaptic density protein 95 in the prefrontal cortex and induced PPI deficits in mature individuals (Ago et al., 2015). In this study, VIPR2 BAC Tg mice showed enhanced locomotor activity, disruption in PPI of the acoustic startle, decrease in social preference, and cognitive impairment (Table 1). These findings suggest that the VPAC2 receptor link to mental health disorders may be due in part to overactive VPAC2 signaling at a time when neural circuits involved in cognition and social behavior are being established. We have shown that activation of the VPAC2 receptor impaired axon outgrowth and decreased dendritic arborization in mouse cortical neurons (Takeuchi et al., 2020). Thus, alternatively or additionally, VPAC2 overactivity may disrupt ongoing synaptic plasticity during the processes of learning and memory.

In the GWAS study, all *VIPR2* microduplications (3 copies) and triplications (4 copies) in the human chromosome 7q36.3 region were located within the *VIPR2* genomic locus or a gene-free

subtelomeric region <89 kb from the transcriptional start site (Vacic et al., 2011). In cultured lymphocytes from patients with 7q36.3 repeats and triplicates, *VIPR2* transcription was increased about two-fold, and the cAMP responses to VIP and a VPAC2 receptor agonist BAY 55-9837 were significantly increased by 30% compared to controls. The exact genetic mechanism for this is unclear. It is likely that duplications of 7q36 affect the regulation of *VIPR2*. Tandem duplication of regulatory sequences, for instance, could affect expression of the gene. Alternatively, the subtelomeric location of *VIPR2* could be relevant to the mechanism. Intrinsic regulation of telomere structure and function affects the transcriptional regulation of adjacent genes, known as telomere position effect (Gottschling et al., 1990; Koering et al., 2002). Together, these findings imply a pathogenic role for increased *VIPR2* gene expression and its downstream signaling in schizophrenia. Our results provide further evidence to support the causal link between *VIPR2* duplication and this disease.

Although there might be a slight difference in the expression levels among brain regions, the VIPR2 BAC Tg mice showed 1.5 to 2-fold increases in the VPAC2 receptor mRNA expression in the brain, indicating the similar changes as seen in cultured lymphocytes from schizophrenic patients with microduplications of 7q36.3. We unexpectedly observed the reductions in PAC1 and VPAC1 receptor expression. The PAC1, VPAC1, and VPAC2 receptors have moderate amino acid sequence similarities (about 50%) with each other and highly three-dimensional structural homology (Laburthe et al., 2007). An endogenous peptide VIP selectively activates VPAC1 and VPAC2, and another PACAP activates all three receptors. Like PAC1 and VPAC1 receptors, VPAC2 couples with Gs-type trimeric G-proteins and activates adenylate cyclase. Thus, any developmental changes or compensatory mechanisms for these PACAP receptors occur in VIPR2 BAC Tg mice, but the exact reasons are still unclear. In humans, the dysregulation of PACAP and the PAC1 receptor has been associated with schizophrenia, depression, and post-traumatic stress disorder (Hashimoto et al., 2007, Hashimoto et al., 2010; Ressler et al., 2011; Mercer et al., 2016; Ross et al., 2020). In mouse primary embryonic cortical neurons, addition of VIP results in a reduction in total numbers and lengths of neuronal dendrites via the VPAC2 receptor, whereas PACAP selectively facilitates the elongation of dendrites via the PAC1 receptor (Takeuchi et al., 2020). To explain these differential effects, it is proposed that VPAC2 and PAC1 signaling undergoes differential timed activations in brain development under normal (physiological) conditions. When the VPAC2 receptor activity is enhanced by *VIPR2* duplications or by pharmacological activation, or if PACAP–PAC1 signaling is reduced by PACAP deficiency, the VPAC2 signaling would be expected to become relatively amplified. This might cause the delay of neural maturation and thus impaired synaptic function, leading to brain dysfunction.

The BAC approach can faithfully reproduce the expression patterns of endogenous human *VIPR2* transgenes in different brain regions with better construct and predictive validity. Furthermore, in the future, the transgene's conditional design and conditional genetic approach will accurately identify pathogenic effects in genetically defined populations of neuronal cell types in different brain regions. Thus, conditional BAC transgenes can provide a novel strategy to model CNVs with copy gain and dissect the pathogenic role of candidate genes by linking their vulnerability to dysfunctional neuronal subtypes and circuits.

Table 1. Summary for the results from the experiments in VIPR2 BAC Tg mice.

Analysis	Function / Target	Experiments	Results (Comparison with wild-type mice)
mRNA expression	PACAP receptors DA-D_2 receptors	Real-time PCR	VPAC2; Increase VPAC1; Decrease PAC1; Decrease DA-D_2; No difference
Behaviors	Sensorimotor gating / Attention	PPI test	Impairment
	Spontaneous locomotor activity	Home-cage activity test in nocturnal and diurnal periods	Increase
	Sociability	Three-chamber social interaction test	Decrease
	Learning and memory	Fear conditioning test	No difference
	Cognition	Novel object recognition test	Impairment

PACAP, pituitary adenylate cyclase-activating polypeptide; PPI, prepulse inhibition; DA, dopamine

1.4 Summary

- We newly generated VIPR2 BAC Tg mice. Southern blot analysis revealed three copies of the transgene in F1 hemizygous mice.
- Expression of VPAC2 receptor mRNA increased in the prefrontal cortex, cerebral cortex, and hippocampus of VIPR2 BAC Tg mice relative to wild-type littermate controls. Expression of PAC1 and VPAC1, but not dopamine-D_2, receptor mRNA in the prefrontal cortex of VIPR2 BAC Tg mice was less than that of wild-type mice.
- VIPR2 BAC Tg mice showed enhanced locomotor activity, disruption in PPI of the acoustic startle, decrease in social preference, and cognitive impairment.

Chapter 2 Development of a selective VPAC2 receptor antagonist peptide

2.1 Background

Worldwide, more than 20 million people suffer from schizophrenia, but effective and definitive new therapeutic drugs/treatments have not been established. The VPAC2 receptor might be an attractive drug target for the treatment of schizophrenia because both preclinical (Ago et al., 2015; Tian et al., 2019) and clinical (Vacic et al., 2011; Levinson et al., 2011; Yuan et al., 2014; Li et al., 2016; Marshall et al., 2017) studies have demonstrated a strong link between high expression/overactivation of the VPAC2 receptor and schizophrenia. Despite these backgrounds, the proof-of-concept of VPAC2 inhibitors has not been examined clinically. A reason might be that the VPAC2 receptor belongs to class-B GPCRs, and the discovery of small-molecule drugs against class-B GPCRs is generally difficult (Hollenstein et al., 2014). Another issue is the structural properties of the VPAC2 receptor. PACAP also binds tightly to its specific receptor PAC1 and high-affinity receptors for VIP, namely VPAC1 and VPAC2 (Harmar et al., 2012; Vaudry et al., 2009). The VPAC2 receptor has about 50% sequence homology with VPAC1 or PAC1 receptors. Therefore, these molecular features have made it difficult to discover VPAC2-selective small molecule drugs (Chu et al., 2010). Under these circumstances, Sakamoto et al. (2018) have constructed large diverse library including 10–100 billion distinct clones displaying various peptide sequences, performed a phage display screening, and then discovered an artificial 16-mer cyclic peptide VIpep-3, Ac-c(CPPYLPRRLC)TLLLRS-OH, which antagonizes human and rodent VPAC2 signaling pathways *in vitro*. VIpep-3 has more than 50-fold receptor selectivity for the VPAC2 receptor compared with the two other receptor subtypes. However, this peptide comprises all-natural amino acids and has high susceptibility to degradation by proteases. *In vivo* efficacy of this VPAC2 receptor antagonist also remains to be determined in animal models of psychiatric disorders such as schizophrenia.

Recently, we performed amino acid substitutions and structural optimization of VIpep-3 and obtained derivatives (Fig. 8). Using structural information of the extracellular domain of VPAC2, the C-terminal structure of VIP, and the docking model of VPAC1/VIP, we constructed a molecular design concept. The amino acid sequence of VIpep-3 is highly conserved in its family except for Arg^{7}, Arg^{8}, Thr^{11}, Leu^{14}, Arg^{15}, and Ser^{16} (Sakamoto et al., 2018). On the basis of the predicted binding mode, it appeared to be better to substitute Arg^{8} with Tyr. Because the three C-terminal residues Leu^{14}, Arg^{15} and Ser^{16} were unlikely to be deeply involved in VPAC2 receptor-binding (Sakamoto et al., 2018), they were deleted. Consequently, the remaining amino acid-substitutable residues were Arg^{7} and Thr^{11}.

A strategy for VIpep-3 structure optimization is introduction of positively charged amino acid L-2,3-diaminopropionic acid (Dap) to the 7th and 11th positions to interact with negatively charged Glu^{34} of the VPAC2 receptor. KS-132, Ac-c(Cys-Pro-Pro-Tyr-Leu-Pro-Dap-Tyr-Leu-Cys)-Dap-Leu-Ile-NH_2 (disulfide bond cyclization with side chains of Cys^1 and Cys^{10}), was designed and synthesized (Fig. 8). Another strategy is bicyclization. For example, VIP analogues Ro 25-1553 (Gourlet et al., 1997) and Ro 25-1392 have been reported as VPAC2-selective agonists that have a cyclic structure by bridging between Lys and Asp. Therefore, we chose bicyclization as another strategy. KS-133, Ac-c[Cys-Pro-Pro-Tyr-Leu-Pro-c(Lys-Tyr-Leu-Cys]-Asp)-Leu-Ile-NH_2 (disulfide bond cyclization with side chains of Cys^1 and Cys^{10}, and amide bond cyclization with side chains of Lys^7 and Asp^{11}), was designed and synthesized.

The aim of this study was thus to generate a VIpep-3 derivative for *in vivo* experiments.

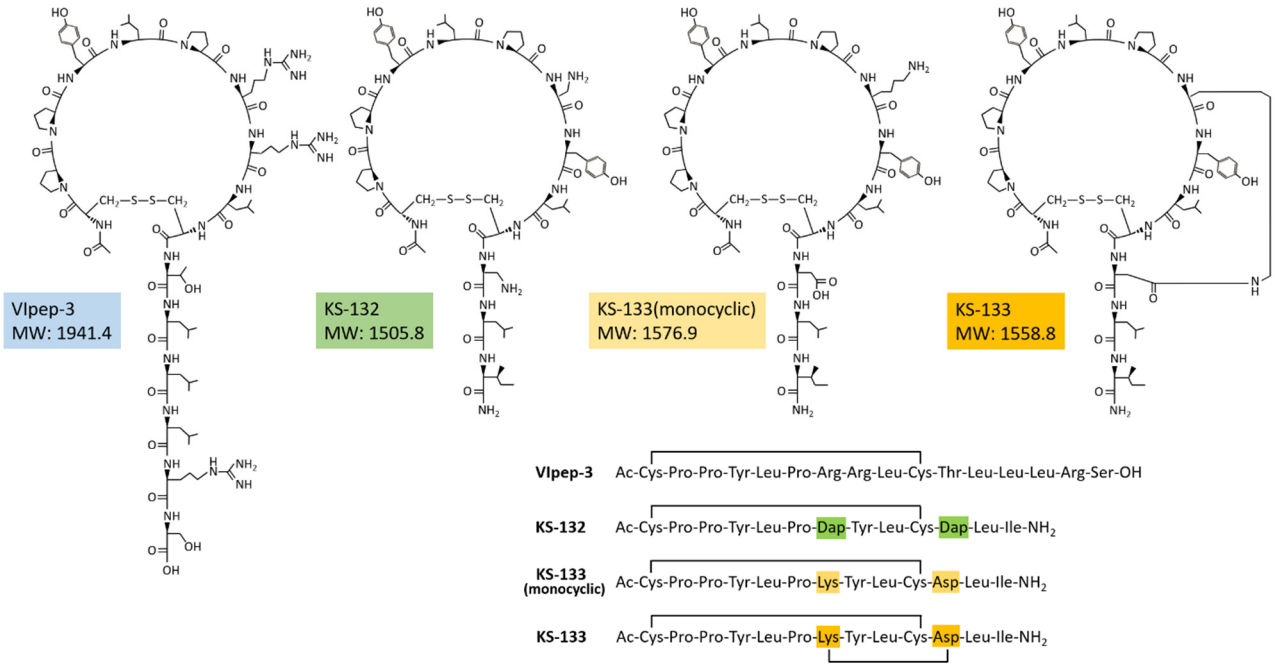

Figure 8. Chemical structures of peptides.

2.2 Results

2.2.1 *In vitro* antagonistic activities of VIpep-3 derivatives towards PACAP receptors

First, the antagonistic activities of parental VIpep-3, KS-132, KS-133(monocyclic) (no bridging between Lys^7 and Asp^{11}), and KS-133 against human VPAC1, VPAC2, and PAC1 receptors were evaluated by a calcium influx assay. After antagonistic peptide treatment for 30 min, ligand at a

concentration of EC_{80} was added to the cells, and then calcium signaling was measured. All peptides antagonized the VIP-VPAC2 signaling pathway in a peptide concentration-dependent manner (Fig. 9) but did not antagonize VIP-VPAC1 and PACAP-PAC1 signaling pathways up to 5 μM (Table 2). KS-132 and KS-133 had IC_{50} values of 33.4 nM and 24.8 nM, respectively, which were stronger antagonistic activities than parental VIpep-3 (40.6 nM) (Table 2).

Next, antagonistic and agonistic activities of KS-133 at the VPAC2 receptor were evaluated by a cAMP assay. As shown in Fig. 9, KS-133 antagonized VIP-VPAC2 signaling pathway in a peptide concentration-dependent manner. The IC_{50} value was determined as 500 nM (Table 2). On the other hand, KS-133 did not exhibit VPAC2 agonist activity, even at a high concentration of 5 μM (Fig. 9 and Table 2).

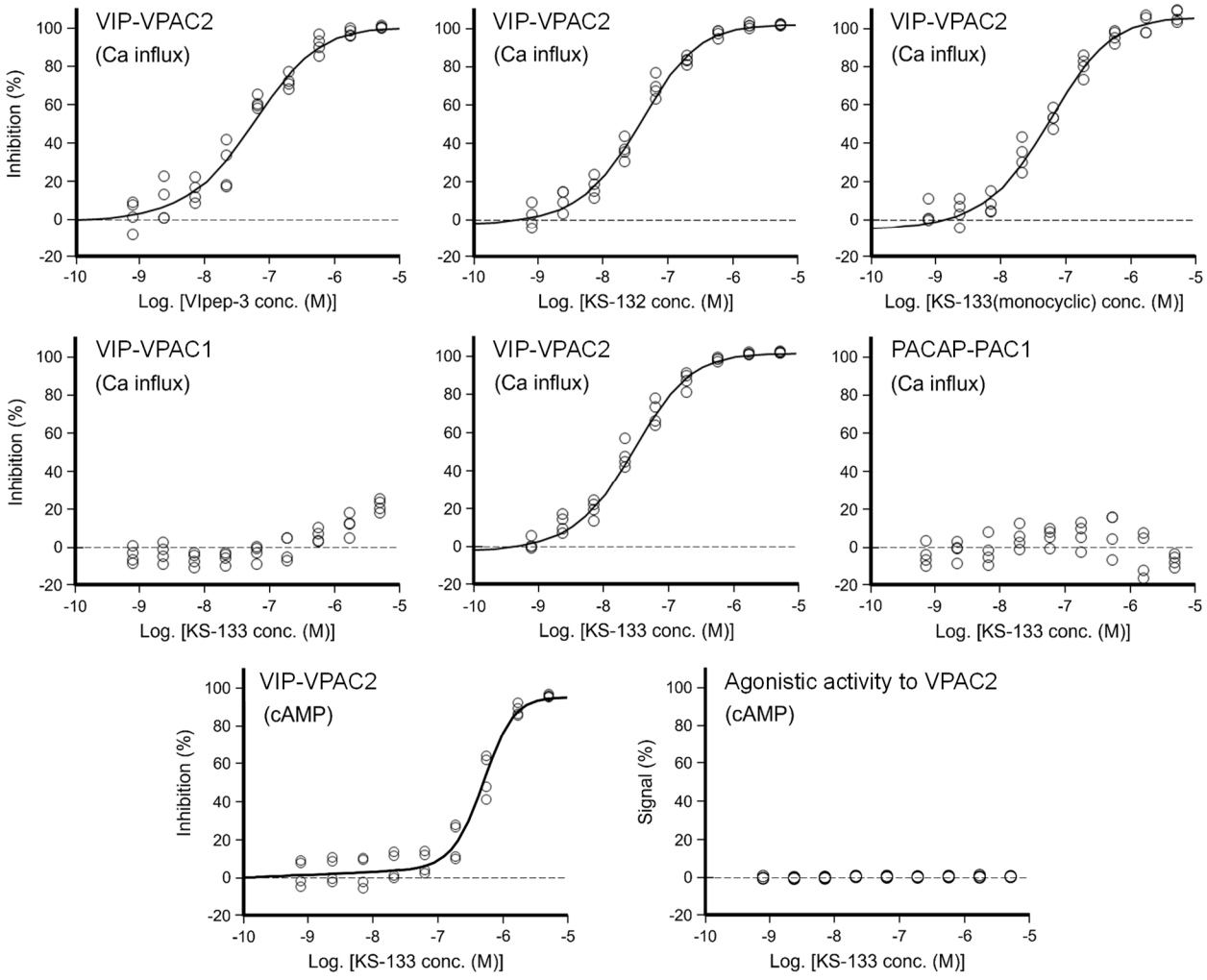

Figure 9. Antagonistic/agonistic activities of peptides in the calcium influx and cAMP assays. For evaluation of the antagonistic activity, the cells were preincubated with antagonistic peptides for 30 min. In the calcium influx assay, after the addition of ligand at EC_{80}, calcium mobilization was monitored immediately (n = 4 wells for each treatment). In the cAMP assay, after a 30-min incubation with the ligand at EC_{80}, cAMP production in cells was measured (n = 4 wells for each treatment).

Table 2. Antagonistic/agonistic activities of peptides in the calcium influx and cAMP assays.

	Ca influx assay [IC_{50} (nM)]			cAMP assay [IC_{50} (nM)]	cAMP assay (nM)
	VIP (25 nM)	VIP (150 nM)	PACAP (35 nM)	VIP (0.5 nM)	Agonistic activity
	VPAC1	VPAC2	PAC1	VPAC2	VPAC2
VIpep-3	> 5,000	40.6 ± 4.0	> 5,000	N.T.	N.T.
KS-132	> 5,000	33.4 ± 2.8	> 5,000	N.T.	N.T.
KS-133(monocyclic)	> 5,000	56.0 ± 3.9	> 5,000	N.T.	N.T.
KS-133	> 5,000	24.8 ± 3.2	> 5,000	500 ± 79	> 5,000

Peptides were tested in the presence of EC_{80} ligand (n = 4 wells, Mean ± SEM). N.T. means not tested.

2.2.2 Resistance to protease degradation of VIpep-3 derivatives

The stability of peptides was evaluated in rat plasma. A peptide was incubated in rat plasma at 37°C for 0 and 24 h, and the remaining amount of peptide was determined by reverse phase-high performance liquid chromatography (RP-HPLC). By comparison with the peak area of the peptide, the remaining amount of the peptide after plasma incubation was estimated. As shown in Table 3, monocyclic peptides VIpep-3 and KS-132 were significantly degraded within 24 h. Conversely, bicyclic peptide KS-133 was highly stable for at least up to 24 h. Interestingly, KS-133(monocyclic) was also highly stable. KS-133(monocyclic) may form a pseudo bicyclic structure by ionic bond interaction between side chains of Lys and Asp.

Table 3. Stabilities of peptides in rat plasma.

Peptide name	Input (N.T.)	Immediately after mixing	Incubation time 24 hrs
VIpep-3	1299273	900813	95354
		100%	10.6%
KS-132	1460241	1206247	696652
		100%	57.8%
KS-133(monocyclic)	768775	744262	724176
		100%	97.3%
KS-133	161695	165254	163537
		100%	99.0%

Peak area values obtained by RP-HPLC and the residual rate (%) are listed.
N.T. indicates no plasma treatment.

2.2.3 *In vivo* VPAC2 receptor antagonistic activity of KS-133

KS-133, which had the most robust antagonistic activity *in vitro* and good resistance to protease degradation, was selected for *in vivo* evaluation. To determine whether KS-133 blocked VPAC2 receptor-mediated signaling in the brain, we first examined the effects of systemic administration of KS-133 on phosphorylation of CREB, a biomarker downstream of the VPAC2 receptor, in neonatal and adult mice (Fig. 10). Subcutaneous administration of the selective VPAC2 receptor agonist Ro 25-1553 (0.4 nmol/g) to ICR mice at P12, when VPAC2 receptors are highly expressed in mouse brain (Waschek et al., 1996), significantly enhanced phosphorylation of CREB in the prefrontal cortex (Fig. 10A). Simultaneous injection of KS-133 (1 nmol/g) suppressed the Ro 25-1553-induced increase in CREB phosphorylation. We also evaluated the effects of KS-133 in adult mice (Fig. 10B). Intranasal administration of the selective VPAC2 receptor agonist BAY 55-9837 (20 μg/mouse) significantly increased phosphorylated CREB in the prefrontal cortex, which was blocked by coadministration of KS-133 (20 nmol/mouse) with BAY 55-9837.

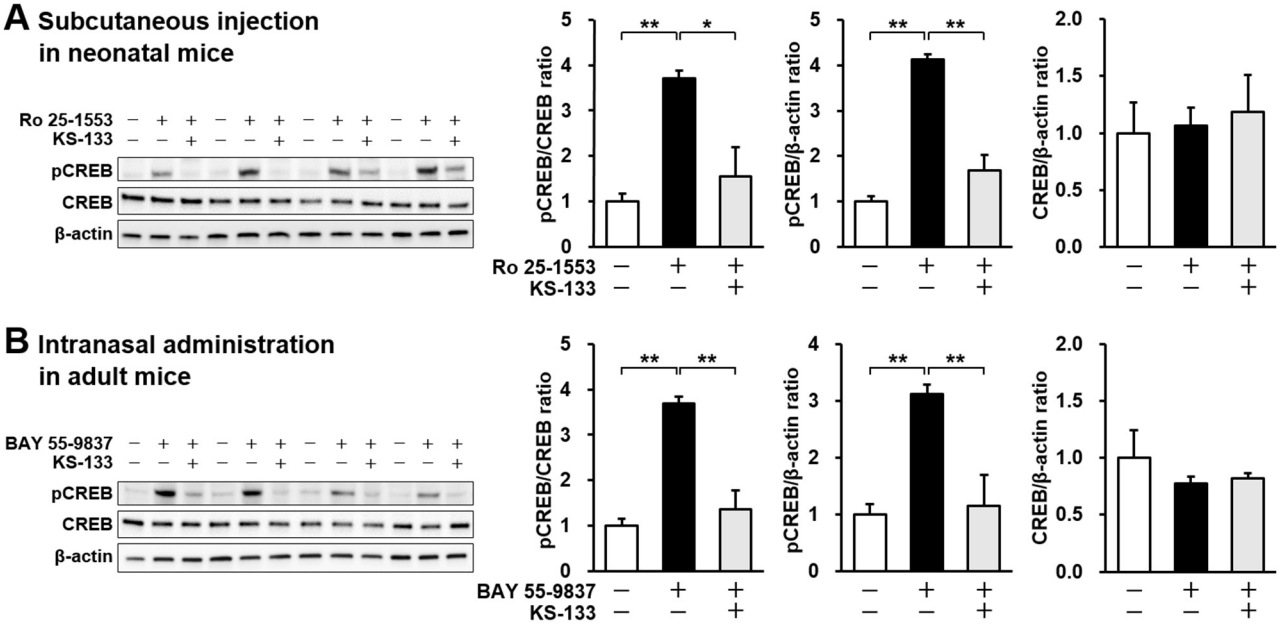

Figure 10. Effects of subcutaneous (A) and intranasal (B) administration of KS-133 on VIPR2 activation-induced phosphorylation of CREB in the prefrontal cortex of mice. Phospho-CREB (pCREB), total CREB, and β-actin levels were analyzed by western blotting. (A) Mice at P12 were s.c. They were Injected with Ro 25-1553 (0.4 nmol/g) or PBS. KS-133 (1 nmol/g) or the vehicle were injected simultaneously into mice. One hour after the injection, the prefrontal cortex of mice was isolated, and pCREB was examined. (B) Mice at eight weeks of age were i.n. they were Injected with BAY 55-9837 (20 μg/mouse) or distilled water. KS-133 (20 nmol/mouse) or the vehicle were injected simultaneously into mice. One hour after the injection, the prefrontal cortex of mice was isolated, and pCREB was examined. Expression levels of pCREB were normalized to total CREB and β-actin. Results are expressed as the mean ± SEM of 4 mice/group. $^{*}P < 0.05$, $^{**}P < 0.01$.

2.2.4 Effects of KS-133 on cognitive impairment in mice

Next, we investigated the pharmacological efficacy of KS-133 in a mouse model of psychiatric disorders on the basis of early postnatal activation of the VPAC2 receptor (Ago et al., 2015) (Fig. 11). Repeated administration of Ro 25-1553 (0.07 nmol/g, s.c., once daily) during P1–14 significantly decreased the difference in time spent exploring each object, whereas PBS-treated control mice explored the novel object by a significant preference in the novel object recognition test (Fig. 11A). Additionally, the discrimination index was significantly lower in mice treated with Ro 25-1553 than in control mice (Fig. 11B). Chronic treatment with KS-133 (1 nmol/g) attenuated the decreases in the difference of time spent exploring each object and cognitive dysfunction. Two-way ANOVA of the discrimination index revealed significant main effects of Ro 25-1553 treatment ($F_{1,63}$ = 17.378, P < 0.0001) and KS-133 treatment ($F_{1,63}$ = 5.261, P < 0.05), and there was a significant interaction between Ro 25-1553 and KS-133 treatments ($F_{1,63}$ = 23.988, P < 0. 0001).

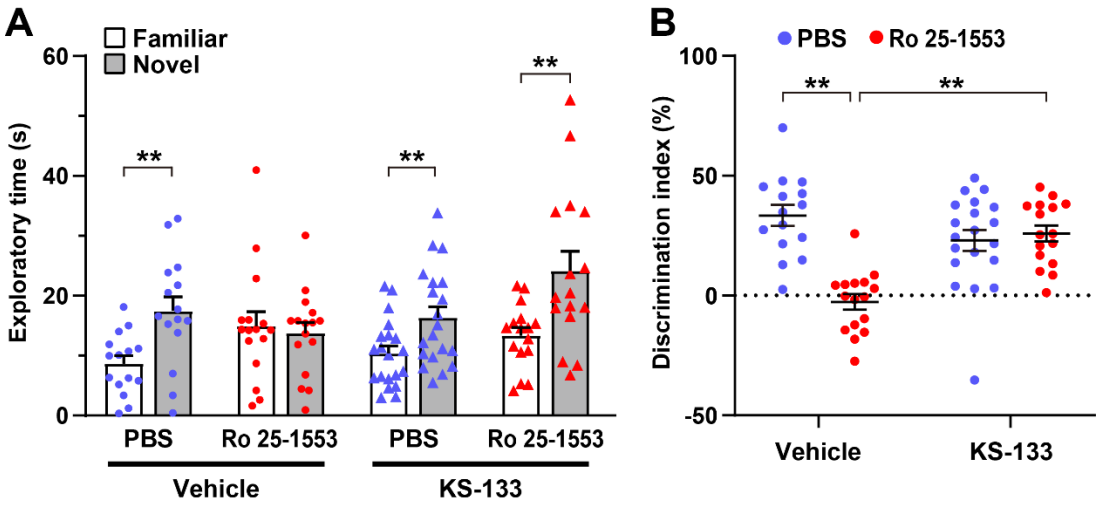

Figure 11. Effects of early postnatal treatment with Ro 25-1553 and KS-133 on recognition memory in the novel object recognition test. Mice were injected s.c. Once-daily with Ro 25-1553 (0.07 nmol/g) or PBS from P1 to P14. KS-133 or the vehicle was simultaneously injected s.c. with Ro 25-1553 or PBS. Then, the novel object recognition test was conducted in adulthood. (A) Time spent exploring each object in the test session. (B) Discrimination index (%) was calculated as the difference between the novel and familiar object exploration times divided by the total time spent exploring the two objects. Results are expressed as the mean ± SEM of 15–20 mice per group. $^{*}P < 0.01$.

2.2.5 Effects of KS-133 on abnormal dendritic morphology in neonatal VPAC2 receptor-activated mice

Because a reduced length of basilar dendrites and a reduced dendritic number have been found in layer 3 in prefrontal cortical areas [Brodmann area (BA) 10, BA 11, and BA 46] and the anterior cingulate cortex (BA 32) of schizophrenic patients (Black et al., 2004; Broadbelt, 2002; Glantz and Lewis, 2000;

Kalus et al., 2000; Konopaske et al., 2014), we examined dendritic morphology in the prefrontal cortex of mice treated with Ro 25-1553 and KS-133 after the novel object recognition test (Fig. 12). Figure 12A shows Golgi-stained pyramidal neurons and representative tracings of soma and dendrites in the prefrontal cortex. Ro 25-1553 reduced the cell soma size, total branch number, and length of apical and basal dendrites of prefrontal cortex neurons (Fig. 12B). These effects were counteracted by simultaneous administration of KS-133 with Ro 25-1553. Sholl analysis also revealed that the amount of dendritic material distal to the soma in apical (treatment × distance interaction: $F_{19, 1482} = 1.957$, $P < 0.01$) and basal ($F_{19, 1482} = 1.750$, $P < 0.05$) dendrites was decreased in Ro 25-1553-treated mice, which indicated a reduction in dendritic complexity. KS-133 prevented the morphological abnormalities in both apical ($F_{19, 1482} = 3.261$, $P < 0.001$) and basal ($F_{19, 1482} = 3.877$, $P < 0.001$) dendrites in the prefrontal cortex.

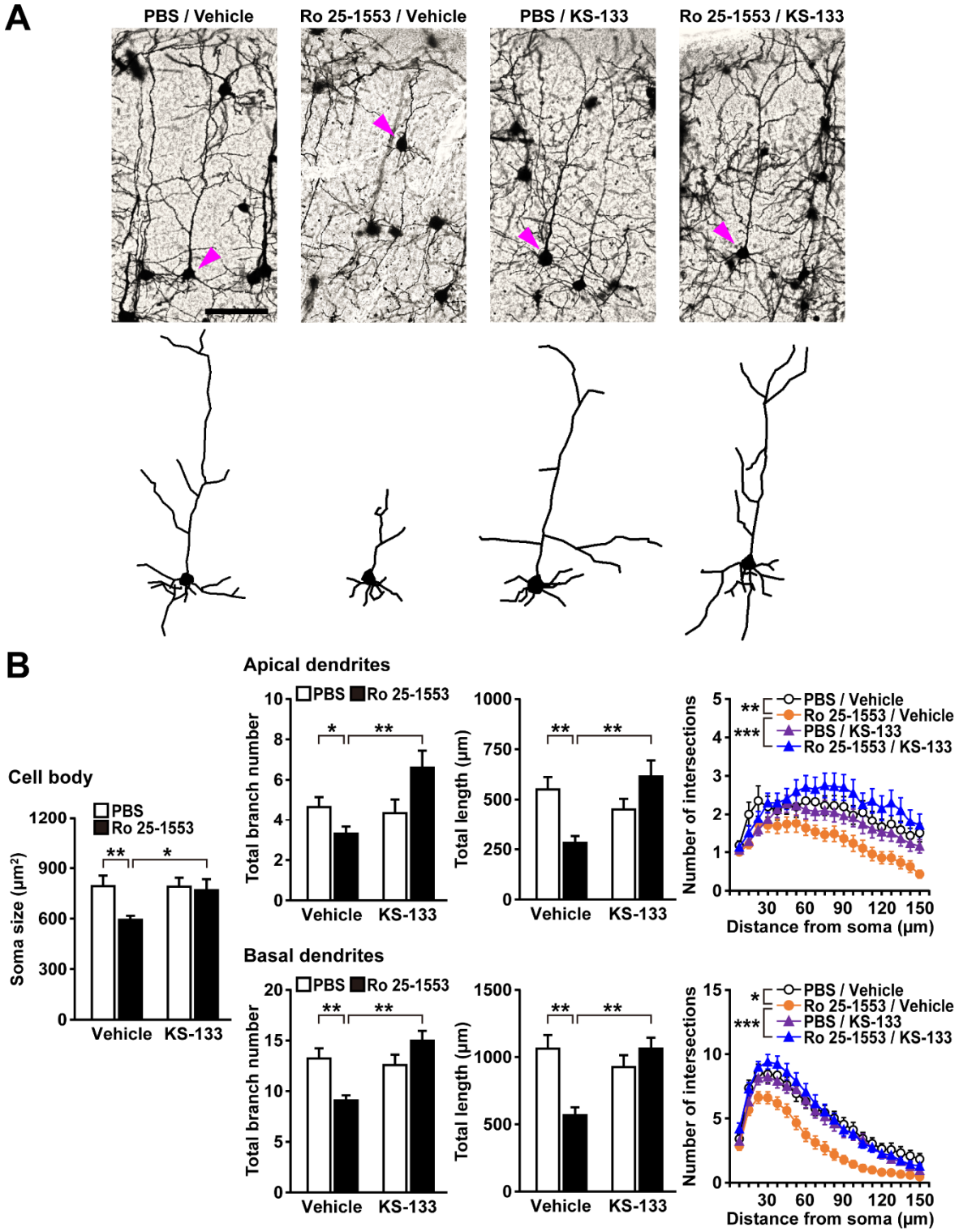

Figure 12. Alterations in the dendritic morphology of prefrontal pyramidal neurons in mice treated with Ro 25-1553 and KS-133 during the early postnatal period. Brain samples were obtained from mice after the novel object recognition test (Fig. 11). (A) Golgi-stained pyramidal neurons and representative tracings of soma and dendrites. Scale = 100 μm. (B) The soma size (area), total branch number, and length of apical and basal dendrites. The number of intersections of dendrites with 7.5-μm concentric spheres centered on the soma was measured by Sholl analysis. Results are expressed as the mean ± SEM of 40 neurons from five mice per group. $^{*}P < 0.05$, $^{**}P < 0.01$, $^{***}P < 0.001$.

2.3 Discussion

A VIpep-3 derivative KS-133 overcame most disadvantages of parental VIpep-3, such as vulnerability to protease degradation, and had high potency and selectivity for the VPAC2 receptor. The VPAC2 receptor antagonist activity was improved in the Gq/calcium signaling pathway (IC_{50} = 25 nM), even though the molecular weight was reduced from VIpep-3 (1941.1 g/mol) to KS-133 (1558.8 g/mol). Bicyclization would stabilize the peptide structure necessary for VPAC2 receptor binding. For the Gs/cAMP signaling pathway, KS-133 showed moderate antagonistic activity (500 nM) against the VPAC2 receptor, whereas it did not exhibit agonist activity. Parental peptide VIpep-3 showed almost equal IC_{50} values in Ca influx assay (47 nM), cAMP assay (33 nM), and β-arrestin assay (<30 nM) (Sakamoto et al., 2018). These data suggest that VIpep-3 has less signaling bias. Because KS-133 has high sequence similarity to VIpep-3, the results from this study might be unexpected. Unfortunately, the crystal structure of the KS-133/VPAC2 receptor complex has not been obtained. The exact reason is unknown, but when a peptide molecule binds to the VPAC2 receptor, a conformational change can occur which impacts subsequent binding of co-regulator proteins and DNA. Importantly, KS-133 is active *in vivo*, inhibiting VPAC2-mediated CREB activation and preventing cognitive impairment in a pharmacological model of early postnatal VPAC2 receptor overactivation, a relevant mouse model of schizophrenia (Ago et al., 2015, 2021).

Generally, drug discovery to target molecules in the CNS is more challenging than in peripheral tissues. Molecule exchange between the periphery and CNS is strictly restricted by the blood−brain barrier (BBB), especially molecules with a molecular weight (MW) of >400 g/mol. In addition to the MW limit, CNS drugs need to have high lipophilicity to cross the BBB (McMartin et al., 1987; Dong, 2018), but high lipophilic small molecules likely have undesirable side effects by potential off-target binding. Conversely, the MW of KS-133 was 1558 g/mol, which would avoid off-target side effects by VPAC2-selective binding but would make it difficult to cross the BBB. In the present study, phosphorylated CREB in the prefrontal cortex of neonatal mice at postnatal day (P) 12 was significantly increased by s.c. Administration of VPAC2 receptor agonist Ro 25-1553, which was suppressed by s.c. co-administration of KS-133. However, it was unclear whether the alterations in CREB phosphorylation were due to direct effects of s.c. injection of Ro 25-1553 and KS-133 on VPAC2 receptors in the CNS. In another experiment, i.n. administration of BAY 55-9837, a VPAC2 receptor agonist, also increased CREB phosphorylation in the prefrontal cortex of adult mice, which was suppressed by i.n. co-administration of KS-133. Intranasal administration is an attractive route for drug delivery to the brain because it allows direct transport of drugs from the nasal cavity to the brain parenchyma by bypassing systemic circulation (Lochhead and Thorne, 2012; Thorne et al., 2004;

Iwasaki et al., 2019). It has been reported that about 1% of an administered molecule enters the CNS without crossing the BBB by the administration to the nasal cavity, even those with an MW of 1000 g/mol (McMartin et al., 1987; Dong, 2018). There are some reports that the BBB becomes leaky in patients with psychiatric disorders such as schizophrenia and ASD (Patel and Frey, 2015; Najjar et al., 2017; Kealy et al., 2020). In the future, to clarify the mechanism and routes of how administered KS-133 targets the CNS, detailed pharmacokinetic studies of KS-133 in healthy mice and disease model mice using s.c., i.n., and intravenous administrations will be needed.

Cognitive deficits are considered a central feature of schizophrenia (Rund, 1998; Green et al., 2000; Bowie and Harvey, 2006). Additionally, clinical studies have shown a relationship between cortical thickness and cognitive performance in frontotemporal brain regions in schizophrenia patients (Alkan et al., 2021), and several different whole-brain voxel-based imaging techniques have identified the medial prefrontal cortex as the main site of abnormality in schizophrenia (Pomarol-Clotet et al., 2010). Thus, in the present study, we focused on recognition memory and dendritic morphology in the prefrontal cortex of early postnatally VPAC2 receptor-activated mice. We found that repeated administration of Ro 25-1553 during P1–14 caused cognitive impairment in adulthood and simultaneous treatment with KS-133 prevented this effect. In agreement with this observation, the same postnatally restricted Ro 25-1553 treatment reduced the total branch number and length of apical and basal dendrites of the prefrontal cortex neurons in mice. Additionally, sholl analysis revealed reductions in dendritic complexity in both apical and basal dendrites. These in vivo morphological abnormalities were counteracted by concomitant administration of KS-133 with Ro 25-1553. Taken together, these findings suggest that activation of the VPAC2 receptor during early postnatal development in mice leads to a long-term impairment of cognition associated with changes in pyramidal cell size and dendritic morphology in the prefrontal cortex and that KS-133 has an *in vivo* VIPR2 antagonistic activity.

2.4 Summary

- KS-133 selectively inhibited VPAC2 receptor-mediated signals *in vitro*.
- Subcutaneous and intranasal administration of KS-133 blocked on phosphorylation of CREB, a biomarker downstream of the VPAC2 receptor, in neonatal and adult mice, respectively.
- KS-133 ameliorated cognitive impairment and abnormal dendritic morphology in a mouse model of psychiatric disorders through early postnatal activation of the VPAC2 receptor.

Conclusion

In the present study, we successfully generated a BAC Tg mouse model of *VIPR2* copy number variation and developed a novel bicyclic peptide KS-133 with a potent and selective VPAC2 receptor antagonist activity that counteracts cognitive decline in a mouse model of psychiatric disorders.

Results of the large-scale genetic studies have demonstrated that rare microduplications at 7q36.3, containing *VIPR2*, encoding the VPAC2 receptor, confer significant risk for schizophrenia and ASD. Lymphocytes from patients with these mutations exhibited higher *VIPR2* gene expression and VIP responsiveness, indicating the functional significance of the microduplications and VPAC2 receptor overactivation (Vacic et al., 2011). While both ligands (VIP and PACAP) appear to play roles in neural cell proliferation, maturation, synaptogenesis, protection, and regeneration (Falluel-Morel et al., 2007; Hill et al., 2007; Passemard et al., 2011), the pathological roles of PACAP and VIP and their mechanistic links to mental health disorders remain largely unknown. VIPR2 BAC Tg mice exhibited enhanced locomotor hyperactivity, sensorimotor-gating deficits, and cognitive impairment. Our studies would provide a useful mouse model for uncovering the causative pathogenic role of *VIPR2* CNV on cognitive circuits and other behavioral manifestations in schizophrenia. We will still need to clearly demonstrate the cell-type-specific and time-dependent effects of VPAC2 receptor overactivation.

KS-133 may contribute to both the development of a novel drug candidate for the treatment of psychiatric disorders such as schizophrenia and the acceleration of fundamental studies on the VPAC2 receptor. Notably, KS-133 had a different mechanism of action (MOA) from existing drugs that are effective mainly for positive symptoms by a common MOA that targets neurotransmitter receptors such as dopamine, serotonin, noradrenaline, and NMDA receptors. Because schizophrenia is a complex multifactorial disease, it is necessary to develop new therapeutic agents on the basis of its pathological mechanism. To further verify the feasibility and validity of drug discovery targeting the VPAC2 receptor in schizophrenia, we will need to examine the effects of KS-133 on behavioral abnormalities in several animal models for schizophrenia as well as VIPR2 BAC Tg mice. Additionally, to clarify the mechanism and routes of how administered KS-133 targets the CNS, detailed pharmacokinetic studies of KS-133 in healthy mice and disease model mice using subcutaneous, intranasal, and intravenous administrations will be needed. After examining the safety and toxicology of KS-133, we hope to proceed with the drug development process such as non-clinical and clinical studies. Because current drug discoveries for the CNS are limited to small compounds, many drug targets of the CNS, such as class-B GPCRs, are considered intractable. Our study might be a practical

example demonstrating that such intractable targets can be druggable targets using a high molecular designed peptide.

Acknowledgments

At the end of this thesis, I would like to express my gratitude to Professor Nakagawa Shinasaku, Graduate School of Pharmaceutical Sciences, Osaka University, and Professor Yukio Ago, Graduate School of Biomedical and Health Sciences, Hiroshima University.

Moreover, to proceed with this research, I have received direct guidance and encouragement, and I would like to thank the Graduate School of Pharmaceutical Sciences, Dr. Kenji Ishimoto and Dr. Nobumasa Hino.

In addition, I would like to thank all of our team members for promoting this research, including Tatsunori Miyaoka, Mei Yamada, Takumi Yamaguchi, Kaiga Katahira, Ryosuke Yamauchi, Shuto Takeuchi, and members of laboratories of Biopharmaceutics and Molecular Neuropharmacology, Graduate School of Pharmaceutical Sciences, Osaka University.

Finally, I am deeply grateful to my parents and Professor Gao Jianqing of the School of Pharmacy, Zhejiang University, and to my predecessors and friends.

The Ph.D. phase has been a process of reinvention and challenge. It is because of the guidance, encouragement, and support that I have been able to achieve my goals step by step. This is the end and the beginning. I will take the rewards with me as I continue to strive to challenge new things, help others and do more meaningful things for society.

2022 .01

Methods

Reagent

Reagent	Company
Tris-HCl (pH 7.5)	#35436-01, Nacalai Tesque, Inc, Kyoto, Japan
2X SDS-PAGE Sample Buffer	#B5834, Tokyo Chemical Industry Co., Ltd, Tokyo, Japan
4%−20% precast gel	#4561096, Bio-Rad Laboratories, Inc., CA
BAY 55-9837 (20 μg/mouse)	Tocris Bioscience, Bristol, UK
Bovine serum albumin	#01863-77, Nacalai Tesque, Inc, Kyoto, Japan
Bromophenol blue	#A2233, Sigma-Aldrich, St. Louis, MO, USA
Can Get Signal™	#NKB-101T; TOYOBO Co., Ltd, Osaka, Japan
CREB (48H2) rabbit monoclonal antibody	#9197, Cell Signaling Technology
Dimethyl sulfoxide (DMSO)	#13445-74, Nacalai Tesque, Inc., Kyoto, Japan
ECL2 Western Blotting Detection Reagents	PerkinElmer, Inc, Waltham, MA
EDTA·2Na	#345-01865, Dojindo Laboratories Kumamoto, Japan
Glycerol	#077-00735, Wako, Ltd. Osaka, Japan
Horseradish peroxidase-conjugated anti-mouse IgG	#ab6789, Abcam, Cambridge, MA
Horseradish peroxidase-conjugated anti-rabbit IgG	#7074, Cell Signaling Technology
Isoflurane	#095-06573, Wako, Ltd. Osaka, Japan
KCl	#000-63435, Kishida Chemical Co., Ltd, Osaka, Japan
NaCl	#31320-05, Nacalai Tesque, Inc, Kyoto, Japan
NP-40	#23640-94, Nacalai Tesque, Inc, Kyoto, Japan
N-PER™ Neuronal Protein Extraction Reagent	#87792, Thermo Fisher Scientific, MA
Phosphatase inhibitor cocktail	#4906845001, Sigma-Aldrich
Phospho-CREB (Ser133) (87G3) rabbit monoclonal antibody	#9198, Cell Signaling Technology, Danvers, MA
Saline	Otsuka Pharma. Co. (Tokushima)
poly-L-arginine	#P7762, Sigma-Aldrich, St. Louis, MO, USA
Ponceau-S Staiining Solution.	#BCL-PSS-01, Beagle. Inc, Kyoto, Japan
Protease inhibitor cocktail	#25955-11, Nacalai Tesque
Ro 25-1553 (0.4 nmol/g)	Peptide Institute, Inc. Osaka, Japan
Skim Milk for immunoassay	#31149-75, Nacalai Tesque, Inc, Kyoto, Japan
Triton-X100	#035501-15, Wako, Ltd. Osaka, Japan
Tween 20	#T0543, Tokyo Chemical Industry Co., Ltd, Tokyo, Japan
β-actin mouse monoclonal antibody	#A2228, Sigma-Aldrich, St. Louis, MO, USA

Ethics statement

Experimental procedures that involved animals and their care were conducted in compliance with the *Guide for the Care and Use of Laboratory Animals* (National Research Council, 1996) and ARRIVE guidelines (McGrath and Lilley, 2015; Kilkenny et al., 2010). All animal experiments were approved by the Animal Care and Use Committee of the Graduate School of Pharmaceutical Sciences, Osaka University (#30-3-2).

Generation of transgenic mice

The BAC construct used for transgenic animal production was obtained from the BACPAC Resources Center at the Children's Hospital of Oakland Research Institute (http://bacpac.chori.org). The selected clone, RP24-386J17 (C57BL/6J background), houses a portion of mouse chromosome 12 inclusive of the full VIPR2 gene, as well as genomic regions both upstream and downstream of the VPAC2 receptor coding sequence. Following purification of the BAC–VIPR2 construct, DNA was injected into pronuclear-stage embryos from C57BL/6J mice (Unitech, Inc., Chiba, Japan). Surviving embryos were implanted into pseudo-pregnant C57BL/6J mice. Progeny were screened for BAC integration by PCR performed using genomic DNA obtained from tail samples with the following primers: forward, 5′-GAACATTTTGAGGCATTTCAGTC-3′, and reverse, 5′-CCACTCATCGCAGTACTGTTGTA-3′. Both primers anneal to sequences within the CmR gene of the bacterial vector. The resulting 588 bp PCR product is therefore only amplified from BAC–VIPR2 positive animals. Only one founder (F0) animal was generated that genotyped positive for multicopy BAC integration. Multiple additional attempts to generate other founders proved unsuccessful.

Southern blot analysis

The copy numbers of the transgene were measured by Southern blot analysis of DNA isolated from the tails of the F1 mice (Unitech, Inc., Chiba, Japan). The copy number of replicates for each individual was calculated based on the concentration of the bands detected in the expected size. At this point, a standard curve was made using the Plasmid DNA containing the probe recognition alignment as a control, and the number of replicates coded into the genome was calculated by numerically assigning the bands to each individual. BAC Tg mice were maintained in their original genetic background (C57BL6/J), and the transgene was transmitted to the offspring from a hemizygous transgenic parent. Wild-type and hemizygous Tg littermates (F2 mice) across multiple litters were used for the experiments.

Real-time RT-PCR

Total RNA was isolated using QIAzol Lysis Reagent (QIAGEN, Tokyo, Japan) according to the manufacturer's protocol. Reverse transcription of total RNA (1 μg) and real-time RT-PCR were performed as described previously (Inoue et al., 2018). Real-time RT-PCR was conducted with GoTaq qPCR Master Mix (Promega, Madison, WI, USA). The following primers were used: 5′-AAGCAAAAACTGCACTAGCGA-3′ (forward) and 5′-GCCCAAGGTATAAATGGCCTTCA-3′

(reverse) for VPAC2; 5′-ATGAGTCTTCCCCAGGTTG-3′ (forward) and 5′-ACCGACAGGTAGTAATAATCC-3′ (reverse) for PAC1; 5′-AGTGAAGACCGGCTACACCA-3′ (forward) and 5′-TCGACCAGCAGCCAGAAGAA-3′ (reverse) for VPAC1; 5′-GGCAAATTCAACGGCACAGT-3′ (forward) and 5′-AGATGGTGATGGGCTTCCC-3′ (reverse) for GAPDH. All data were normalized to GAPDH mRNA levels and expressed as the relative change in mRNA.

Experiment animals

Pregnant ICR (CD1) mice at 16 days of gestation and male C57BL/6J mice at 7 weeks of age were purchased from Japan SLC Inc. (Shizuoka, Japan). Mice were housed individually in plastic cages under a standard 12-h light/dark cycle (lights on 08:00 hours) at a constant temperature of 22 ± 1°C. The animals had ad libitum access to food and water. Pregnant females were monitored for the parturition date that was considered as postnatal day (P) 0.

Synthetic peptides

VIpep-3, KS-132, KS-133(monocyclic) (no bridging between Lys^{7} and Asp^{11}), and KS-133 were synthesized at SCRUM Inc. (Tokyo, Japan) using Fmoc-based solid-phase peptide synthesis, followed by reverse phase-high performance liquid chromatography (RP-HPLC) purification. Peptide purity was ascertained by analytical RP-HPLC and the structural assignment was performed by matrix-assisted laser desorption ionization-time of flight mass spectrometry (MALDI-TOF MS).

Drug administration

For western blot analysis, ICR neonatal mice at P12 (7–10 g body weight) were administered subcutaneously (s.c.) with KS-133 (1 nmol/g) and Ro 25-1553 (0.4 nmol/g), a selective VPAC2 agonist (Gourlet et al., 1997; Harmar et al., 2012), and adult C57BL/6J mice at 8 weeks of age (20–30 g body weight) were intranasally (i.n.) injected with KS-133 (20 nmol/mouse) and BAY 55-9837 (20 μg/mouse), another selective VPAC2 agonist (Tsutsumi et al., 2002; Tian et al., 2019). The dosages of these drugs were determined in a preliminary experiment using the change in phosphorylation of CREB as an index. Ro 25-1553 was dissolved in phosphate-buffered saline (PBS) and BAY 55-9837 was dissolved in distilled water. KS-133 was dissolved in saline with 1% dimethyl sulfoxide (DMSO) for s.c. injection or saline with 5% DMSO and 5 mg/mL poly-L-arginine for i.n. injection. The volumes of the drug solutions were 5 mL/kg body weight for s.c. injection and 10 μL for i.n. injection.

For behavioral experiments, all litters were randomly divided into Ro 25-1553- and PBS-treated groups. From P1 to P14, mice were injected s.c. once daily with Ro 25-1553 at a dose of 0.07 nmol/g (Ago et al., 2015). Mice treated with PBS from P1 to P14 were used as the control. KS-133 or the vehicle was simultaneously injected with Ro 25-1553 or PBS. Animals were weaned at P21 and divided by gender at P28. We used male mice exclusively to minimize any potential variability due to sex-specific effects on behavioral performance. All groups were derived from at least four different litters to preclude possible differences in individual maternal behaviors as a mitigating factor in any

subsequent long-lasting changes induced in the offspring. Behavioral analyses of mice were carried out at 2−3 months of age. Experimenters were blinded to the treatment while testing.

Western blot analysis

We anesthetized each mouse with isoflurane, removed their brain rapidly, dissected the prefrontal cortex on ice, frozen it on dry ice, then kept it at −80°C until analysis.N-PER™ Neuronal Protein Extraction Reagent was used to homogenize tissue samples with a protease inhibitor cocktail and phosphatase inhibitor cocktail at 4°C. Incubation on ice for 30 minutes was followed by centrifugation at 14,000×*g* for 15 minutes at 4°C, which collected the supernatant. Forty-five (phospho-CREB and CREB) protein was loaded onto a 4%−20% precast gel, separated by sodium dodecyl sulfate-polyacrylamide electrophoresis, and then transferred electrophoretically to a hydrophobic polyvinylidene fluoride membrane. The blotted membranes were blocked with a blocking buffer (5% bovine serum albumin in Tris-buffered saline with 0.1% Tween-20) for 1 h at room temperature and then incubated with primary antibodies phospho-CREB (Ser133) (87G3) rabbit monoclonal antibody (1:500), CREB (48H2) rabbit monoclonal antibody (1:1000) at 4°C overnight. An anti-rabbit IgG-conjugated horseradish peroxidase (1:3000) was then added to the membranes. The primary and secondary antibodies were diluted with Can Get Signal™ Solution 1 and 2, respectively. The immune complexes were visualized using ECL2 Western Blotting Detection Reagents. Densitometric analysis was performed with the software package CS analyzer 4. Expression levels of phospho-CREB were normalized to CREB. The results are expressed as fold changes relative to the PBS/vehicle-treated control group.

Novel object recognition test

The novel object recognition test was carried out in accordance with previous reports (Hara et al., 2016; Takuma et al., 2014). In brief, after habituation to the experimental box under dim light conditions (30 lx) for 3 consecutive days, the test mouse was allowed to freely explore two novel objects (A and B) placed in the box for 10 min. Twenty-four hours after the training session, the retention session was conducted. In the retention session, object B was replaced with novel object C and the mouse was allowed to move freely for 5 min in the same box. The exploration time for each object in the retention session was measured with a stopwatch. The discrimination index (%) was the difference between the exploration time for the novel object plus that for the familiar object divided by the total exploration time. This index was used to calculate values for recognition memory. This test was conducted between 9:00–15:00.

Acoustic startle test—prepulse inhibition (PPI)

Acoustic startle responses were measured in a startle chamber (SR-LAB®; San Diego Instruments, San Diego, CA), based on previous studies with slight modifications (Ishihama et al., 2010; Koda et al., 2008; Yano et al., 2009). A moderate light environment was used in the chamber (240 lx), during which the animals were exposed to 65 dB of white noise for 10 minutes. The test procedure consisted of a startling test (40 ms of 120 dB white noise), a no-stimulus test (background noise only), and a PPI

test a 120 dB startle pulse (40 ms) preceded by a prepulse (20 ms of a white noise pulse of 75, 80 or 85 dB intensity) for 100 ms. Trials were pseudo-randomized with trial intervals between 7 and 23 s (mean: 15 s), ensuring that each trial was presented 20 times. Each animal received a total of 100 trials, and the whole procedure lasted approximately 30 minutes. Spontaneous activity during the no-stimulus trials was 10-20 (any unit). After starting the startle stimulus, startle responses were recorded for 100 ms (responses were measured every 1 ms). During the 100-ms sampling window, the startle amplitude was used as the dependent variable. For each prepulse trial type, the PPI was calculated as a percentage score. PPI (%) = (1-[(startle response for pulses with prepulse)/(startle response for pulses alone)]) × 100

Three-chambered social interaction test

A three-room arena measuring 41 cm long × 60 cm wide × 23.5 cm high was used to assess social skills (Ago et al., 2015). As the subject mice were black, white plexiglass panels were mounted on the back wall, and the entire arena was placed on a white plexiglass floor to provide a contrasting background. The two outside rooms contained an inverted black empty wire cup containing the stimulated mice. The laboratory was lit by standard fluorescent lamps (5 lx), and tests were performed from 10:00 to 16:00. Intruder mice were selected from C57BL/6J male mice of the same age that had never met. Mice were assessed for social competence in a three-chamber apparatus. Briefly, during a 10-min adaptation period, one subject mouse was placed in the middle chamber, the sliding door was opened, and the mouse was given free access to the entire arena. During that time, the mice were manually scored with a stopwatch for the length of time they spent in the two external stimulus compartments. At the end of the habituation phase, the mice were placed back in the center, the door was closed, and an unfamiliar male C57BL/6J mouse was placed in one of the two cups. Time spent in each chamber was measured over a period of 10 min, and the amount of time spent in each chamber was examined to determine how much time was spent in each chamber by the test mice.

Fear condition test

All fear condition tests were conducted using four identical fear conditioning chambers (30 cm × 24 cm × 21 cm, Med Associates Inc., St. Albans, VT), as previously reported (Ago et al., 2015), equipped with the Med Associates video freezing system. Day 1 of tone conditioning in the conditioning chamber (Context A) consisted of a 150 s baseline period followed by five tones (30 s, 2.8 kHz, 80 dB) paired with electric shocks (2 s, 0.5 mA), starting immediately after the offset presented by each tone, with a 90 s trial interval between the end of each shock and the start of the next tone. Freezing was recorded during the baseline period and each tone period. Twenty-four hours later (day 2), mice were placed in the same conditioning chamber (context A) for an 8-minute contextual fear test. There was no stimulation during this period. Freezing was recorded throughout the 8-minute test. On day 3 of the cued fear test, mice were placed in a chamber with a triangular ceiling with a dark roof and grid floor covering (Context B) and allowed to explore the new environment for 150 s before being presented with five tones (30 s, 2.8 kHz, 80 dB), each with a 90-s trial interval. Freezing was recorded during the baseline period and each tone period. Twenty-four hours after the cued fear test, the

extinction phase began in Context B. After a 3-min exploration, mice were exposed to 20 tones (30 s, 2.8 kHz, 80 dB) for two consecutive days (days 4 and 5), with a 5s inter-trial interval each day. The mice were removed from the chamber 3 minutes after the last cue presentation. Freezing was recorded at the baseline period and each tone period. Data are expressed as a four-step average of each of the five tones.

Spontaneous locomotor activity

One mouse was placed in a transparent test cage (24 cm × 17 cm × 12 cm), and the voluntary momentum was measured in the compartment using a SUPERMEX® momentum measuring device (Muromachi Kikai Co., Ltd., Tokyo). Using Supermex, the temperature was 22 ± 1 ° C, the light was turned on at 8:00, and the light and darkness were switched every 12 hours, and the amount of voluntary exercise was measured for one week in an environment where food and water could be freely drawn. The amount of activity during the daytime and at nighttime was analyzed.

Histology and dendritic analyses

After the novel object recognition test, dendritic morphological analysis was performed on mice, and samples were collected within 10 minutes after dissection. As reported previously (Ago et al., 2017; Hara et al., 2016), Golgi-Cox impregnation was carried out using an FD Rapid Golgi Stain™ Kit. Using isoflurane to sedate the mice, their brains were removed, rinsed with Milli-Q water, and immersed in a solution that contained potassium dichromate, mercuric chloride, and potassium chromate. In a cryoprotectant solution, the brains were stored in the dark for 72 hours after being stored at room temperature for two weeks. The impregnated brains were embedded in 3.5% agarose gel and cut with a vibratome (VT1000S; Leica Microsystems) at room temperature. Coronal sections of 100 μm in thickness were mounted on Gelatin-Coated Microscope Slides and dried in air at room temperature in the dark for 24 h. After drying, the sections were rinsed with Milli-Q water, reacted in the working solution, and dehydrated with a 50%, 75%, 95%, and 100% graded ethanol series. Finally, the sections were dewaxed in xylene and coverslipped using Mount Quick. Digitized images from the prefrontal cortex (+2.245 through +1.345 mm concerning the bregma) (Dong, 2018a) were obtained under an upright light microscope with a cooled CCD digital camera system (Axio Imager.M2/AxioCam MRc5; Carl Zeiss, Jena, Germany). A 20× lens was used to measure dendrites. For analysis, we retained only fully impregnated neurons with intact dendritic trees that were isolated from neighboring fully impregnated neurons. Forty pyramidal neurons with the soma in layers II/III were selected from four mice per group in the prefrontal cortex. The apical and basal dendrites' morphology was quantified in three dimensions using the Neurolucida neuron tracing system (MBF Bioscience, Williston, VT) with the experimenter blinded to the treatment. We compared the length and number of branches of apical and basal dendrites between treatments. Sholl analysis was performed using a NeuroExplorer (MBF Bioscience) to assess dendritic material differences in the amount and location.

Calcium influx and cAMP assays

Evaluation of antagonist activities of peptides against VIP-VPAC1, VIP-VPAC2, and PACAP-PAC1 signaling pathways and agonistic activity of KS-133 at VPAC2 was carried out by Eurofins DiscoverX (Fremont, CA, USA). Intracellular calcium mobilization was monitored using a calcium-sensitive dye loaded in CHO-K1 cells expressing human VPAC1 (ITEM 86-0030P-2243AN), VPAC2 (ITEM 86-0030P-2244AN), and PAC1 (ITEM 86-0030P-2066AN). The cells were preincubated with antagonistic peptides for 30 min at room temperature in the dark. After the addition of the ligand at EC_{80}, calcium mobilization was immediately monitored by FLIPR Tetra for 2 min. Cyclic AMP production in CHO-K1 cells expressing human VPAC2 was evaluated using HitHunter® cAMP assays (antagonist mode: ITEM 86-0007P-2362AN; agonist mode: ITEM 86-0007P-2362AG). The cells were preincubated with antagonistic peptides for 30 min at room temperature. After the addition of the ligand at EC_{80}, cells were further incubated for 30 min at room temperature. Cells were lysed, and the cAMP content of the cell lysate was determined by the β-galactosidase-based enzyme fragment complementation assay (Eglen, 2002). IC_{50} values were estimated by the following equation: IC50 = 10^[Log(A/B) × (50 – D)/(C – D) + Log(B)], where A is the concentration at >50% inhibition, B is the concentration at <50% inhibition, C is the inhibition rate at concertation A, and D is the inhibition rate at concertation B.

Evaluation of peptide stability in rat plasma

Each peptide (10 mM, 1 μL) was incubated with rat plasma (20 μL) prepared in-house. Immediately after mixing with plasma and after 24 h of incubation at 37°C, 80% acetonitrile (200 μL) was added to extract VIpep-3, and acetonitrile (200 μL) was added to extract KS-132, KS-133(monocyclic), and KS-133. The mixture was stored for 10 min on ice and then centrifuged at 20,000×g for 10 min at 4°C. The supernatant was recovered and directly applied to RP-HPLC to determine the remaining amount of unmodified peptides in the sample.

Statistical analysis

All data are expressed as the mean ± standard error of the mean (SEM). Data from western blots were analyzed using one-way analysis of variance (ANOVA), followed by the Tukey–Kramer *posthoc* test. For behaviors, the total number of dendrites, and dendritic length, data were analyzed using Student's *t*-test or two-way ANOVA, followed by the Tukey–Kramer test. For sholl analysis, data were analyzed using two-way ANOVA with drug treatment as the intersubject factor and repeated measures with distance from the soma as the intrasubject factor. Statistical analyses were conducted using the software package StatView® 5.0 for Windows (SAS Institute, Cary, NC). A value of $P < 0.05$ was considered statistically significant.

References

Ago, Y., Asano, S., Hashimoto, H., & Waschek, J. A. (2021). Probing the *VIPR2* Microduplication Linkage to Schizophrenia in Animal and Cellular Models. *Frontiers in Neuroscience, 15*, 717490-717490. doi:10.3389/fnins.2021.717490

Ago, Y., Condro, M. C., Tan, Y. V., Ghiani, C. A., Colwell, C. S., Cushman, J. D., . . . Waschek, J. A. (2015). Reductions in synaptic proteins and selective alteration of prepulse inhibition in male C57BL/6 mice after postnatal administration of a VIP receptor (*VIPR2*) agonist. *Psychopharmacology (Berl), 232*(12), 2181-2189. doi:10.1007/s00213-014-3848-z

Ago, Y., Hayata-Takano, A., Kawanai, T., Yamauchi, R., Takeuchi, S., Cushman, J. D., . . . Waschek, J. A. (2017). Impaired extinction of cued fear memory and abnormal dendritic morphology in the prelimbic and infralimbic cortices in VPAC2 receptor (*VIPR2*)-deficient mice. *Neurobiology of learning and memory, 145*, 222-231. doi:10.1016/j.nlm.2017.10.010

Alkan, E., Davies, G., & Evans, S. L. (2021). Cognitive impairment in schizophrenia: relationships with cortical thickness in fronto-temporal regions, and dissociability from symptom severity. *NPJ schizophrenia, 7*(1), 20-20. doi:10.1038/s41537-021-00149-0

Amann, L. C., Gandal, M. J., Halene, T. B., Ehrlichman, R. S., White, S. L., McCarren, H. S., Siegel, S. J. (2010). Mouse behavioral endophenotypes for schizophrenia. *Brain Res Bull, 83*(3-4), 147-161. doi: 10.1016/j.brainresbull.2010.04.008

An, S., Tsai, C., Ronecker, J., Bayly, A., & Herzog, E. D. (2012). Spatiotemporal distribution of vasoactive intestinal polypeptide receptor 2 in mouse suprachiasmatic nucleus. *The Journal of Comparative Neurology, 520*(12), 2730-2741. doi:10.1002/cne.23078

Black, J. E., Kodish, I. M., Grossman, A. W., Klintsova, A. Y., Orlovskaya, D., Vostrikov, V., . . . Greenough, W. T. (2004). Pathology of layer V pyramidal neurons in the prefrontal cortex of patients with schizophrenia. *The American journal of psychiatry, 161*(4), 742-744. doi:10.1176/appi.ajp.161.4.742

Bowie, C. R., & Harvey, P. D. (2006). Cognitive deficits and functional outcome in schizophrenia. *Neuropsychiatric disease and treatment, 2*(4), 531-536. doi:10.2147/nedt.2006.2.4.531

Broadbelt, K. (2002). Evidence for a decrease in basilar dendrites of pyramidal cells in schizophrenic medial prefrontal cortex. *Schizophrenia Research, 58*(1), 75-81. doi:10.1016/s0920-9964(02)00201-3

Chu, A., Caldwell, J. S., & Chen, Y. A. (2010). Identification and characterization of a small molecule antagonist of human VPAC(2) receptor. *Mol Pharmacol, 77*(1), 95-101. doi:10.1124/mol.109.060137

Dong, X. (2018). Current Strategies for Brain Drug Delivery. *Theranostics, 8*(6), 1481-1493. doi:10.7150/thno.21254

Eglen, R. M. (2002). Enzyme fragment complementation: a flexible high throughput screening assay technology. *Assay Drug Dev Technol 1*, 97-104. doi: 10.1089/154065802761001356

Falluel-Morel, A., Chafai, M., Vaudry, D., Basille, M., Cazillis, M., Aubert, N., et al. (2007). The neuropeptide pituitary adenylate cyclase-activating polypeptide exerts anti-apoptotic and differentiating effects during neurogenesis: focus on cerebellar granule neurones and embryonic stem cells. *J Neuroendocrinol, 19*, 321-327. doi: 10.1111/j.1365-2826.2007.01537.x

Fett, A. K., Viechtbauer, W., Dominguez, M. D., Penn, D. L., van Os, J., Krabbendam, L. (2011). The relationship between neurocognition and social cognition with functional outcomes in schizophrenia: a meta-analysis. *Neurosci Biobehav Rev, 35*(3), 573-588. doi: 10.1016/j.neubiorev.2010.07.001

Feuk, L., Carson, A. R., & Scherer, S. W. (2006). Structural variation in the human genome. *Nature Reviews Genetics, 7*(2), 85-97. doi:10.1038/nrg1767

Foley, C., Corvin, A., Nakagome, S. (2017). Genetics of Schizophrenia: Ready to Translate? *Curr Psychiatry Rep 19(9)*, 61. doi: 10.1007/s11920-017-0807-5

Glantz, L. A., & Lewis, D. A. (2000). Decreased Dendritic Spine Density on Prefrontal Cortical Pyramidal Neurons in Schizophrenia. *Archives of General Psychiatry, 57*(1), 65. doi:10.1001/archpsyc.57.1.65

Gottschling, D. E., Aparicio, O. M., Billington, B. L., Zakian, V. A. (1990). Position effect at S. cerevisiae telomeres: reversible repression of Pol II transcription. *Cell, 63*(4), 751-762. doi: 10.1016/0092-8674(90)90141-z

Gourlet, P., Vertongen, P., Vandermeers, A., Vandermeers-piret, M.-C., Rathe, J., De Neef, P., . . . Robberecht, P. (1997). The Long-Acting Vasoactive Intestinal Polypeptide Agonist RO 25-1553 Is Highly Selective of the VIP 2 Receptor Subclass. *Peptides, 18*(3), 403-408. doi:10.1016/s0196-9781(96)00322-1

Green, M. F., Kern, R. S., Braff, D. L., & Mintz, J. (2000). Neurocognitive Deficits and Functional Outcome in Schizophrenia: Are We Measuring the "Right Stuff"? *Schizophrenia Bulletin, 26*(1), 119-136. doi:10.1093/oxfordjournals.schbul.a033430

Hanks, A. N., Dlugolenski, K., Hughes, Z. A., Seymour, P. A., Majchrzak, M. J. (2013). Pharmacological disruption of mouse social approach behavior: relevance to negative symptoms of schizophrenia. *Behav Brain Res, 252*, 405-414. doi: 10.1016/j.bbr.2013.06.017

Hara, Y., Ago, Y., Taruta, A., Katashiba, K., Hasebe, S., Takano, E., . . . Takuma, K. (2016). Improvement by methylphenidate and atomoxetine of social interaction deficits and recognition memory impairment in a mouse model of valproic acid-induced autism. *Autism Research, 9*(9), 926-939.

Harmar, A. J., Fahrenkrug, J., Gozes, I., Laburthe, M., May, V., Pisegna, J. R., . . . Said, S. I. (2012). Pharmacology and functions of receptors for vasoactive intestinal peptide and pituitary adenylate cyclase-activating polypeptide: IUPHAR review 1. *British Journal of Pharmacology, 166*(1), 4-17. doi:10.1111/j.1476-5381.2012.01871.x

Harmar, A. J., Marston, H. M., Shen, S., Spratt, C., West, K. M., Sheward, W. J., et al. (2002). The VPAC2 receptor is essential for circadian function in the mouse suprachiasmatic nuclei. *Cell, 109*, 497-508. doi: 10.1016/s0092-8674(02)00736-5

Harvey, P. D., Keefe, R. S. (2001). Studies of cognitive change in patients with schizophrenia following novel antipsychotic treatment. *The American Journal of Psychiatry, 158*(2), 176-184. doi: 10.1176/appi.ajp.158.2.176

Hashimoto, R., Hashimoto, H., Shintani, N., Chiba, S., Hattori, S., Okada, T., . . . Baba, A. (2007). Pituitary adenylate cyclase-activating polypeptide is associated with schizophrenia. *Molecular Psychiatry, 12*(11), 1026-1032. doi: 10.1038/sj.mp.4001982

Hashimoto, R., Hashimoto, H., Shintani, N., Ohi, K., Hori, H., Saitoh, O., . . . Kunugi H. (2010). Possible association between the pituitary adenylate cyclase-activating polypeptide (PACAP)

gene and major depressive disorder. *Neuroscience Letters, 468*(3): 300-302. doi: 10.1016/j.neulet.2009.11.019

Hill, J. M. (2007). Vasoactive intestinal peptide in neurodevelopmental disorders: therapeutic potential. *Current Pharmaceutical Design, 13*(11), 1079-1089. doi:10.2174/138161207780618975

Hollenstein, K., de Graaf, C., Bortolato, A., Wang, M.-W., Marshall, F. H., & Stevens, R. C. (2014). Insights into the structure of class B GPCRs. *Trends in Pharmacological Sciences, 35*(1), 12-22. doi:10.1016/j.tips.2013.11.001

Holt, D. J., Lebron-Milad, K., Milad, M. R., Rauch, S. L., Pitman, R. K., Orr, S. P., Cassidy, B. S., Walsh, J. P., Goff, D. C. (2009). Extinction memory is impaired in schizophrenia. *Biological Psychiatry, 65*(6), 455-463. doi: 10.1016/j.biopsych.2008.09.017

Inoue, N., Ogura, S., Kasai, A., Nakazawa, T., Ikeda, K., Higashi, S., Isotani, A., Baba, K., Mochizuki, H., Fujimura, H., Ago, Y., Hayata-Takano, A., Seiriki, K., Shintani, Y., Shintani, N., Hashimoto, H. (2018). Knockdown of the mitochondria-localized protein p13 protects against experimental parkinsonism. *EMBO Reports 19*(3), e44860. doi: 10.15252/embr.201744860

Ishihama, T., Ago, Y., Shintani, N., Hashimoto, H., Baba, A., Takuma, K., & Matsuda, T. (2010). Environmental factors during early developmental period influence psychobehavioral abnormalities in adult PACAP-deficient mice. *Behavioural Brain Research, 209*(2), 274-280. doi:10.1016/j.bbr.2010.02.009

Iwasaki, S., Yamamoto, S., Sano, N., Tohyama, K., Kosugi, Y., Furuta, A., . . . Amano, N. (2019). Direct Drug Delivery of Low-Permeable Compounds to the Central Nervous System Via Intranasal Administration in Rats and Monkeys. *Pharmaceutical Research, 36*(5). doi:10.1007/s11095-019-2613-8

Kalus, P., Muller, T. J., Zuschratter, W., & Senitz, D. (2000). The Dendritic Architecture of Prefrontal Pyramidal Neurons in Schizophrenic Patients.pdf. *Neuroeport, 11*(16), 3621-3625. doi:10.1097/00001756-200011090-00044

Kealy, J., Greene, C., & Campbell, M. (2020). Blood-brain barrier regulation in psychiatric disorders. *Neuroscience Letters, 726*, 133664. doi:10.1016/j.neulet.2018.06.033

Keefe, R. S., Bilder, R. M., Davis, S. M., Harvey, P. D., Palmer, B. W., Gold, J. M., Meltzer, H. Y., Green, M. F., Capuano, G., Stroup, T. S., McEvoy, J. P., Swartz, M. S., Rosenheck, R. A., Perkins, D. O., Davis, C. E., Hsiao, J. K., Lieberman, J. A.; CATIE Investigators; Neurocognitive Working Group. (2007). Neurocognitive effects of antipsychotic medications in patients with chronic schizophrenia in the CATIE Trial. *Arch Gen Psychiatry, 64*(6), 633-647. doi: 10.1001/archpsyc.64.6.633

Kilkenny, C., Browne, W., Cuthill, I. C., Emerson, M., & Altman, D. G. (2010). Animal research: reporting in vivo experiments: the ARRIVE guidelines. *British Journal of Pharmacology, 160*(7), 1577-1579.

Koda, K., Ago, Y., Kawasaki, T., Hashimoto, H., Baba, A., & Matsuda, T. (2008). Galantamine and donepezil differently affect isolation rearing-induced deficits of prepulse inhibition in mice. *Psychopharmacology (Berl), 196*(2), 293-301. doi:10.1007/s00213-007-0962-1

Koering, C. E., Pollice, A., Zibella, M. P., Bauwens, S., Puisieux, A., Brunori, M., . . . Gilson, E. (2002). Human telomeric position effect is determined by chromosomal context and telomeric chromatin integrity. *EMBO Reports*, *3*(11), 1055-1061. doi: 10.1093/embo-reports/kvf215

Konopaske, G. T., Lange, N., Coyle, J. T., & Benes, F. M. (2014). Prefrontal cortical dendritic spine pathology in schizophrenia and bipolar disorder. *JAMA Psychiatry, 71*(12), 1323-1331. doi:10.1001/jamapsychiatry.2014.1582

Kushima, I., Aleksic, B., Nakatochi, M., Shimamura, T., Okada, T., Uno, Y., . . . Ozaki, N. (2018). Comparative Analyses of Copy-Number Variation in Autism Spectrum Disorder and Schizophrenia Reveal Etiological Overlap and Biological Insights. *Cell Reports, 24*(11), 2838-2856. doi:10.1016/j.celrep.2018.08.022

Laburthe, M., Couvineau, A., Tan, V. (2007). Class II G protein-coupled receptors for VIP and PACAP: structure, models of activation and pharmacology. *Peptides, 28*, 1631-1639. doi: 10.1016/j.peptides.2007.04.026

Levinson, D. F., Duan, J., Oh, S., Wang, K., Sanders, A. R., Shi, J., . . . Gejman, P. V. (2011). Copy number variants in schizophrenia: confirmation of five previous findings and new evidence for 3q29 microdeletions and VIPR2 duplications. *The American Journal of Psychiatry, 168*(3), 302-316. doi:10.1176/appi.ajp.2010.10060876

Li, Z., Chen, J., Xu, Y., Yi, Q., Ji, W., Wang, P., Shen, J., Song, Z., . . . Shi, Y. (2016). Genome-wide Analysis of the Role of Copy Number Variation in Schizophrenia Risk in Chinese. *Biological Psychiatry, 80*(4), 331-337. doi:10.1016/j.biopsych.2015.11.012

Lochhead, J. J., & Thorne, R. G. (2012). Intranasal delivery of biologics to the central nervous system. *Advanced Drug Delivery Reviews, 64*(7), 614-628. doi:10.1016/j.addr.2011.11.002

Malhotra, D., & Sebat, J. (2012). CNVs: harbingers of a rare variant revolution in psychiatric genetics. *Cell, 148*(6), 1223-1241. doi:10.1016/j.cell.2012.02.039

Marshall, C. R., Howrigan, D. P., Merico, D., Thiruvahindrapuram, B., Wu, W., Greer, D. S., . . . Schizophrenia Working Groups of the Psychiatric Genomics, C. (2017). Contribution of copy number variants to schizophrenia from a genome-wide study of 41,321 subjects. *Nature Genetics, 49*(1), 27-35. doi:10.1038/ng.3725

McGrath, J. C., & Lilley, E. (2015). Implementing guidelines on reporting research using animals (ARRIVE etc.): new requirements for publication in BJP. *British Journal of Pharmacology, 172*(13), 3189-3193. doi:10.1111/bph.12955

McMartin, C., Hutchinson, L. E. F., Hyde, R., & Peters, G. E. (1987). Analysis of Structural Requirements for the Absorption of Drugs and Macromolecules from the Nasal Cavity. *Journal of Pharmaceutical Sciences, 76*(7), 535-540. doi:10.1002/jps.2600760709

Mena, A., Ruiz-Salas, J. C., Puentes, A., Dorado, I., Ruiz-Veguilla, M., & De la Casa, L. G. (2016). Reduced Prepulse Inhibition as a Biomarker of Schizophrenia. *Frontiers in Behavioral Neuroscience, 10*, 202-202. doi:10.3389/fnbeh.2016.00202

Mercer, K. B., Dias, B., Shafer, D., Maddox, S. A., Mulle, J. G., Hu, P., Walton, J., Ressler, K. J. (2016). Functional evaluation of a PTSD-associated genetic variant: estradiol regulation and *ADCYAP1R1*. *Translational Psychiatry, 6*(12), e978. doi: 10.1038/tp.2016.241

Millan, M. J., Andrieux, A., Bartzokis, G., Cadenhead, K., Dazzan, P., Fusar-Poli, P., . . . Weinberger, D. (2016). Altering the course of schizophrenia: progress and perspectives. *Nat Rev Drug Discov, 15*(7), 485-515. doi:10.1038/nrd.2016.28

Najjar, S., Pahlajani, S., De Sanctis, V., Stern, J. N. H., Najjar, A., & Chong, D. (2017). Neurovascular Unit Dysfunction and Blood-Brain Barrier Hyperpermeability Contribute to Schizophrenia

Neurobiology: A Theoretical Integration of Clinical and Experimental Evidence. *Frontiers in Psychiatry, 8*, 83-83. doi:10.3389/fpsyt.2017.00083

National Research Council (1996). *Guide for the Care and Use of Laboratory Animals*. Washington, DC: National Academy Press, doi: 10.17226/5140

Nestler, E. J., & Hyman, S. E. (2010). Animal models of neuropsychiatric disorders. *Nature Neuroscience, 13*(10), 1161-1169. doi:10.1038/nn.2647

Owen, M. J., Sawa, A., & Mortensen, P. B. (2016). Schizophrenia. *Lancet (London, England), 388*(10039), 86-97. doi:10.1016/S0140-6736(15)01121-6

Passemard, S., Sokolowska, P., Schwendimann, L., Gressens, P. (2011). VIP-induced neuroprotection of the developing brain. *Curr Pharm Des, 17*(10), 1036-1039. doi: 10.2174/138161211795589409

Patel, J. P., & Frey, B. N. (2015). Disruption in the Blood-Brain Barrier: The Missing Link between Brain and Body Inflammation in Bipolar Disorder? *Neural plasticity, 2015*, 708306-708306. doi:10.1155/2015/708306

Pomarol-Clotet, E., Canales-Rodríguez, E. J., Salvador, R., Sarró, S., Gomar, J. J., Vila, F., . . . McKenna, P. J. (2010). Medial prefrontal cortex pathology in schizophrenia as revealed by convergent findings from multimodal imaging. *Molecular Psychiatry, 15*(8), 823-830. doi:10.1038/mp.2009.146

Ressler, K. J., Mercer, K. B., Bradley, B., Jovanovic, T., Mahan, A., Kerley, K., . . . May V. (2011). Post-traumatic stress disorder is associated with PACAP and the PAC1 receptor. *Nature, 470*(7335), 492-497. doi: 10.1038/nature09856

Ross, R. A., Hoeppner, S. S., Hellberg, S. N., O'Day, E. B., Rosencrans, P. L., Ressler, K. J., May, V., Simon, N. M. (2020). Circulating PACAP peptide and PAC1R genotype as possible transdiagnostic biomarkers for anxiety disorders in women: a preliminary study. *Neuropsychopharmacology, 45*(7), 1125-1133. doi: 10.1038/s41386-020-0604-4

Rosti, R. O., Sadek, A. A., Vaux, K. K., & Gleeson, J. G. (2013). The genetic landscape of autism spectrum disorders. *Developmental Medicine & Child Neurology, 56*(1), 12-18. doi:10.1111/dmcn.12278

Rund, B. R. (1998). A Review of Longitudinal Studies of Cognitive Functions in Schizophrenia Patients. *Schizophrenia Bulletin, 24*(3), 425-435. doi:10.1093/oxfordjournals.schbul.a033337

Sakamoto, K., Koyama, R., Kamada, Y., Miwa, M., & Tani, A. (2018). Discovery of artificial VIPR2-antagonist peptides possessing receptor- and ligand-selectivity. *Biochemical and Biophysical Research Communications, 503*(3), 1973-1979. doi:10.1016/j.bbrc.2018.07.144

Sharma, T., Antonova, L. (2003). Cognitive function in schizophrenia. Deficits, functional consequences, and future treatment. *Psychiatr Clin North Am, 26*(1), 25-40. doi: 10.1016/s0193-953x(02)00084-9

Shen, S., Spratt, C., Sheward, W. J., Kallo, I., West, K., Morrison, C. F., et al. (2000). Overexpression of the human VPAC2 receptor in the suprachiasmatic nucleus alters the circadian phenotype of mice. *Proc Natl Acad Sci U S A, 97*(21), 11575-11580. doi: 10.1073/pnas.97.21.11575

Sheward, W. J., Lutz, E. M., Harmar, A. J. (1995). The distribution of vasoactive intestinal peptide2 receptor messenger RNA in the rat brain and pituitary gland as assessed by in situ hybridization. *Neuroscience, 67*(2), 409-418. doi: 10.1016/0306-4522(95)00048-n

Silverman, J. L., Yang, M., Lord, C., Crawley, J. N. (2010). Behavioural phenotyping assays for mouse models of autism. *Nat Rev Neurosci, 11*(7), 490-502. doi: 10.1038/nrn2851

Takeuchi, S., Kawanai, T., Yamauchi, R., Chen, L., Miyaoka, T., Yamada, M., . . . Ago, Y. (2020). Activation of the VPAC2 Receptor Impairs Axon Outgrowth and Decreases Dendritic Arborization in Mouse Cortical Neurons by a PKA-Dependent Mechanism. *Frontiers in Neuroscience, 14*, 521-521. doi:10.3389/fnins.2020.00521

Takuma, K., Hara, Y., Kataoka, S., Kawanai, T., Maeda, Y., Watanabe, R., . . . Matsuda, T. (2014). Chronic treatment with valproic acid or sodium butyrate attenuates novel object recognition deficits and hippocampal dendritic spine loss in a mouse model of autism. *Pharmacology Biochemistry and Behavior, 126*, 43-49. doi:10.1016/j.pbb.2014.08.013

Thorne, R. G., Pronk, G. J., Padmanabhan, V., & Frey, W. H. (2004). Delivery of insulin-like growth factor-I to the rat brain and spinal cord along olfactory and trigeminal pathways following intranasal administration. *Neuroscience, 127*(2), 481-496. doi:10.1016/j.neuroscience.2004.05.029

Tian, X., Richard, A., El-Saadi, M. W., Bhandari, A., Latimer, B., Van Savage, I., . . . Lu, X. H. (2019). Dosage sensitivity intolerance of VIPR2 microduplication is disease causative to manifest schizophrenia-like phenotypes in a novel BAC transgenic mouse model. *Mol Psychiatry, 24*(12), 1884-1901. doi:10.1038/s41380-019-0492-3

Tsutsumi, M., Claus, T. H., Liang, Y., Li, Y., Yang, L., Zhu, J., . . . Pan, C. Q. (2002). A Potent and Highly Selective VPAC2 Agonist Enhances Glucose-Induced Insulin Release and Glucose Disposal: A Potential Therapy for Type 2 Diabetes. *Diabetes, 51*(5), 1453-1460. doi:10.2337/diabetes.51.5.1453

Vacic, V., McCarthy, S., Malhotra, D., Murray, F., Chou, H.-H., Peoples, A., . . . Sebat, J. (2011). Duplications of the neuropeptide receptor gene VIPR2 confer significant risk for schizophrenia. *Nature, 471*(7339), 499-503. doi:10.1038/nature09884

Vaudry, D., Falluel-Morel, A., Bourgault, S., Basille, M., Burel, D., Wurtz, O., . . . Vaudry, H. (2009). Pituitary Adenylate Cyclase-Activating Polypeptide and Its Receptors: 20 Years after the Discovery. *Pharmacological Reviews, 61*(3), 283-357. doi:10.1124/pr.109.001370

Walsh, T., McClellan, J. M., McCarthy, S. E., Addington, A. M., Pierce, S. B., Cooper, G. M., . . . Sebat, J. (2008). Rare Structural Variants Disrupt Multiple Genes in Neurodevelopmental Pathways in Schizophrenia. *Science (New York, N.Y.), 320*(5875), 539-543. doi:10.1126/science.1155174

Waschek, J. A., Ellison, J., Bravo, D. T., & Handley, V. (1996). Embryonic expression of vasoactive intestinal peptide (VIP) and VIP receptor genes. *Journal of Neurochemistry, 66*(4), 1762-1765.

Yano, K., Koda, K., Ago, Y., Kobayashi, H., Kawasaki, T., Takuma, K., & Matsuda, T. (2009). Galantamine improves apomorphine-induced deficits in prepulse inhibition via muscarinic ACh receptors in mice. *British Journal of Pharmacology, 156*(1), 173-180.

Young, J. W., Powell, S. B., Risbrough, V., Marston, H. M., Geyer, M. A. (2009). Using the MATRICS to guide development of a preclinical cognitive test battery for research in schizophrenia. *Pharmacol Ther, 122*(2), 150-202. doi: 10.1016/j.pharmthera.2009.02.004

Yuan, J., Jin, C., Sha, W., Zhou, Z., Zhang, F., Wang, M., . . . Wang, J. (2014). A competitive PCR assay confirms the association of a copy number variation in the VIPR2 gene with schizophrenia in Han Chinese. *Schizophrenia Research, 156*(1), 66-70. doi:10.1016/j.schres.2014.04.004